

STUDY OF HEAT AND MASS TRANSFER EFFECTS ON UNSTEADY FREE CONVECTIVE MHD FLOW IN POROUS MEDIUM

This chapter deals with heat and mass transfer effects on MHD flow through porous medium. Like the heat transfer, mass transfer is also one of the areas of modern science. Heat and mass transfer processes appears in several branches of modern technology, particularly, in atomic power engineering, space research, power plant, industrial power engineering, chemical engineering, construction industry, etc.

This chapter consists of two section, the first one deals with the study of heat and mass transfer characteristics in the unsteady natural convective MHD Casson fluid flow passing through an oscillating vertical plate in porous medium whereas in second section, effects of heat and mass transfer on MHD flow of Second grade fluid in porous medium with ramped boundary conditions is considered.

3.1 SECTION I: HEAT AND MASS TRANSFER IN MHD CASSON FLUID FLOW PAST AN OSCILLATING VERTICAL PLATE EMBEDDED IN POROUS MEDIUM WITH RAMPED WALL TEMPERATURE

In this section, detailed discussion of effects of heat and mass transfer on unsteady MHD flow of Casson fluid past an oscillating vertical plate embedded in porous medium with ramped wall temperature. In order to understand the effects of ramped wall temperature, the said problem is also discussed for isothermal temperature. For both thermal plates, the governing system of linear partial differential equations with imposed initial boundary conditions are solved analytically using the best fitted Laplace transform technique and obtained expression of velocity, temperature and concentration profiles. The features of the fluid flow, heat and mass transfer characteristics are analyzed by plotting graphs and the physical aspects are discussed in details. Expression for Sherwood number, Nusselt number and Skin friction are derived and presented in tabular form (Refer Table 3.1.1 to 3.1.5).

3.1.1 Introduction of the problem

The characteristics of flow in modern engineering are not understandable with the Newtonian fluid model. Hence, non-Newtonian fluid theory can be used instead of Newtonian fluid. Non-Newtonian fluid exerts non-linear relationships between the shear stress and rate of shear strain. It has an

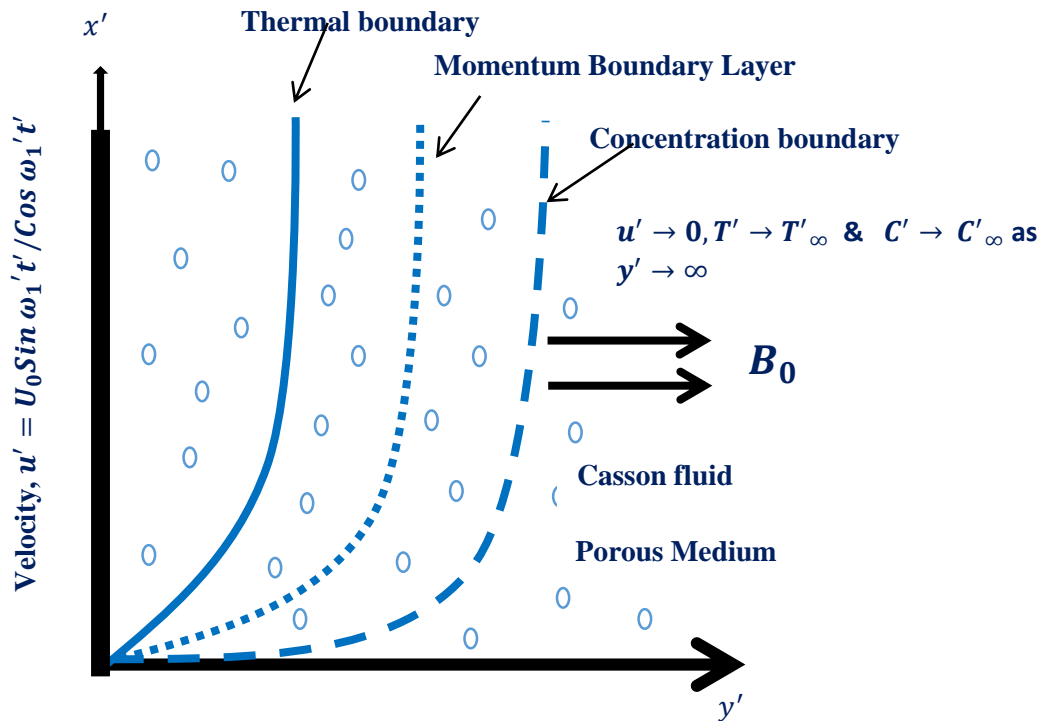
extensive variety of applications in engineering and industry, especially in the extraction of crude oil from petroleum products. Lots of other fluids also have the similar types of characteristics but Casson fluid is one of the time independent non-Newtonian fluids which classified as the most popular non-Newtonian fluid which has several applications in food processing and bio-engineering operations. Casson fluid model first introduced by Casson [7] for the prediction of the flow behavior of pigment-oil suspensions. Pramanik [31] studied Casson fluid flow past an exponentially porous stretching surface.

In nature, there are many flows exist which are produced not only by the temperature differences but also by concentration differences. These mass transfer differences do affect the rate of heat transfer. This phenomenon of heat and mass transfer often occurs in the processes of chemical industries such as, food processing and polymer production. Recently, Khan et al. [63], Kataria and Mittal [96-97] and Khan et al. [122] studied heat and mass transfer effects on unsteady MHD flow of nano fluid. On the other hand, flow of porous media has an important application in heat removal from nuclear fuel, debris, underground disposal of radioactive waste material and paper production etc. Ali et al. [85] studied conjugate effects of heat and mass transfer on MHD free convection flow in porous medium. Ahmed et al. [104] obtained numerical solution of MHD radiating heat and mass transfer in a Darcian porous regime. Nayak et al. [112] considered heat and mass transfer effects on MHD viscoelastic fluid over a stretching sheet through porous medium. In all the previous study, the results for fluid flow problems are found by assuming conditions for the fluid temperature at the plate as continuous and well defined, but there are numerous physical conditions where the temperature at the bounding surface may need non-uniform or arbitrary wall conditions. Lee and Yovanovich [140] considered effects of step change in wall temperature on free convection from vertical plate. Applications of ramped wall type temperature are also found in materials processing, turbine blade heat transfer and electronic circuits operations. Seth et al. [142-147] discussed free convective unsteady MHD flow with ramped temperature whereas Nandkeolyar et al. [152] defined the solution of free convective MHD dusty fluid flow past an impulsively moving vertical plate with ramped wall temperature. Presently many researchers like, Nadeem et al. [46], Akabar et al. [47-48] and Nadeem et al. [88] studied unsteady free convective MHD Casson fluid flow with different physical conditions.

3.1.2 Novelty of the problem

The study by Khalid et al. [89] highlighted unsteady MHD free convection flow of Casson fluid past over an oscillating vertical plate embedded in a porous medium without considering mass transfer and ramped boundary conditions effects. So, present study takes mass transfer effects on unsteady free convective MHD Casson fluid flow past over an oscillating vertical plate with ramped wall temperature and isothermal temperature in consideration. The governing dimensionless equations are solved analytically using Laplace transform technique. Also expression for Skin friction, Nusselt number and Sherwood number are derived.

3.1.3 Mathematical formulation of the problem



$$T' = \begin{cases} T'_\infty + (T'_w - T'_\infty) t'/t_0 & \text{if } 0 < t' < t_0 \\ T'_w & \text{if } t' \geq t_0 \end{cases} \quad \& \quad C' = C'_\infty + (C'_w - C'_\infty) t'/t_0 \quad \text{as } t' > 0 \text{ as } y' = 0$$

Figure 3.1.1: Physical sketch of the problem.

In Figure. 3.1.1, the flow being confined to $y' > 0$, where y' measured in the normal direction to the plate and x' -axis along the wall in the upward direction. A uniformly transverse magnetic field B_0 is applied in the y' direction. Induced magnetic field produced by the fluid motion is negligible

in comparison with the applied one as the magnetic Reynolds number is small enough to neglect the effects of applied magnetic field. Initially, at time $t' = 0$, both the fluid and the plate are uniform temperature T'_∞ and the concentration near the plate is assumed to be C'_∞ respectively. At time $t' > 0$, the plate begins to oscillate in its own plate according to $U_0 \sin(\omega_1 t')$ or $U_0 \cos(\omega_1 t')$ with constant heat flux, $T'_\infty + (T'_w + T'_\infty) t'/t_0$ when $t' < t_0$ and T'_w when $t' > t_0$ respectively and Concentration near the plate is raised linearly to $C'_\infty + (C'_w + C'_\infty) t'/t_0$ which is there after maintained constant T'_w and C'_w respectively.

Before deriving equation, it is assumed that flow is incompressible and one dimensional. Further it is assumed that viscous dissipation term in the energy equation is neglected. Under these assumptions, the following partial differential equations is obtained.

$$\rho \frac{\partial u'}{\partial t'} = \mu\beta \left(1 + \frac{1}{\gamma}\right) \frac{\partial^2 u'}{\partial y'^2} - \sigma B_0^2 u' - \frac{\mu\phi}{k'} u' + \rho g \beta'_T (T' - T'_\infty) + \rho g \beta'_C (C' - C'_\infty) \quad (3.1.1)$$

$$\frac{\partial T'}{\partial t'} = \frac{k_4}{\rho c_p} \frac{\partial^2 T'}{\partial y'^2} \quad (3.1.2)$$

$$\frac{\partial C'}{\partial t'} = D_M \frac{\partial^2 C'}{\partial y'^2} \quad (3.1.3)$$

$$u' = 0, T' = T'_\infty, C' = C'_\infty; \text{ as } y' \geq 0 \text{ and } t' \leq 0,$$

$$u' = U_0 \sin(\omega_1 t') \text{ or } U_0 \cos(\omega_1 t'), T' = \begin{cases} T'_\infty + (T'_w - T'_\infty) t'/t_0 & \text{if } 0 < t' < t_0 \\ T'_w & \text{if } t' \geq t_0 \end{cases} \text{ and}$$

$$C' = C'_\infty + (C'_w - C'_\infty) t'/t_0 \text{ as } t' > 0 \text{ and } y' = 0$$

$$u' \rightarrow 0, T' \rightarrow T'_\infty, C' \rightarrow C'_\infty; \text{ as } y' \rightarrow \infty \text{ and } t' \geq 0 \quad (3.1.4)$$

Introducing the following dimensionless quantities:

$$y = \frac{U_0}{\nu t_0} y', t = \frac{U_0^2 t'}{\nu t_0}, u = \frac{\sqrt{t_0}}{U_0} u', \theta = \frac{(T' - T'_\infty)}{(T'_w - T'_\infty)}, C = \frac{(C' - C'_\infty)}{(C'_w - C'_\infty)}, \omega_1 = \frac{\omega_1' \nu}{U_0^2}, Pr = \frac{\rho \nu c_p}{k_4}, \tau = \frac{\tau}{\rho u^2}$$

$$M^2 = \frac{\sigma B_0^2 t_0}{\rho U_0^2}, \frac{1}{k} = \frac{\nu \phi^2}{k' U_0^2}, Gr = \frac{\nu g \beta'_T (T'_w - T'_\infty)}{U_0^3}, \gamma = \frac{\mu \beta \sqrt{2\pi c}}{P_y}, Sc = \frac{\nu}{D_M}, Gm = \frac{\nu g \beta'_C (C'_w - C'_\infty)}{U_0^3}$$

In the equations (3.1.1) to (3.1.4) dropping out the " ' " notation (for simplicity)

$$\frac{\partial u}{\partial t} = \left(1 + \frac{1}{\gamma}\right) \frac{\partial^2 u}{\partial y^2} - \left(M^2 + \frac{1}{k}\right) u + G_r \theta + G_m C \quad (3.1.5)$$

$$\frac{\partial \theta}{\partial t} = \frac{1}{Pr} \frac{\partial^2 \theta}{\partial y^2} \quad (3.1.6)$$

$$\frac{\partial C}{\partial t} = \frac{1}{s_c} \frac{\partial^2 C}{\partial y^2} \quad (3.1.7)$$

with initial and boundary conditions

$$u = \theta = C = 0, \quad y > 0, t < 0$$

$$u = \sin(\omega_1 t) \text{ or } H(t) \cos(\omega_1 t),$$

$$\theta = \begin{cases} t, & 0 < t \leq 1 \\ 1 & t > 1 \end{cases} = tH(t) - (t-1)H(t-1), \quad C = t \text{ at } y = 0, t \geq 0$$

$$u \rightarrow 0, \theta \rightarrow 0, C \rightarrow 0 \quad \text{at } y \rightarrow \infty \quad (3.1.8)$$

Where, H(.) is Heaviside unit step function.

3. 1.4 Solution of the problem

Using Laplace transform technique, expression for velocity, temperature and concentration are obtained from equations (3.1.5) to (3.1.7) with initial and boundary conditions as in equation (3.1.8).

3.1.4.1 Solution for plate with ramped wall temperature

Taking Laplace transform of equations (3.1.5) and (3.1.7) with initial and boundary condition equations (3.1.8)

$$\bar{\theta} = (1 - e^{-s})F_8(y, s) \quad (3.1.9)$$

$$\bar{C} = F_{11}(y, s) \quad (3.1.10)$$

$$\bar{u}_{sin}(y, s) = \frac{i}{2}F_1(y, s) - \frac{i}{2}F_2(y, s) + (1 - e^{-s})G_1(y, s) - (1 - e^{-s})G_2(y, s) + G_3(y, s) - G_4(y, s) \quad (3.1.11)$$

$$\bar{u}_{cos}(y, s) = \frac{1}{2}F_1(y, s) + \frac{1}{2}F_2(y, s) + (1 - e^{-s})G_1(y, s) - (1 - e^{-s})G_2(y, s) + G_3(y, s) - G_4(y, s) \quad (3.1.12)$$

$$G_1(y, s) = a_1F_3(y, s) + a_2F_4(y, s) + a_3F_5(y, s) \quad (3.1.13)$$

$$G_2(y, s) = a_1F_6(y, s) + a_2F_7(y, s) + a_3F_8(y, s) \quad (3.1.14)$$

$$G_3(y, s) = a_4F_4(y, s) + a_5F_5(y, s) + a_6F_9(y, s) \quad (3.1.15)$$

$$G_4(y, s) = a_4 F_{10}(y, s) + a_5 F_{11}(y, s) + a_6 F_{12}(y, s) \quad (3.1.16)$$

$$G_5(y, t) = a_3 F_4(y, t) - a_3 F_3(y, t) \quad (3.1.17)$$

$$G_6(y, t) = a_3 F_7(y, t) - a_3 F_6(y, t) \quad (3.1.18)$$

$$F_1(y, s) = \frac{e^{-y\sqrt{\frac{s+b}{a}}}}{s+i\omega_1} \quad (3.1.19)$$

$$F_2(y, s) = \frac{e^{-y\sqrt{\frac{s+b}{a}}}}{s-i\omega_1} \quad (3.1.20)$$

$$F_3(y, s) = \frac{e^{-y\sqrt{\frac{s+b}{a}}}}{s-f} \quad (3.1.21)$$

$$F_4(y, s) = \frac{e^{-y\sqrt{\frac{s+b}{a}}}}{s} \quad (3.1.22)$$

$$F_5(y, s) = \frac{e^{-y\sqrt{\frac{s+b}{a}}}}{s^2} \quad (3.1.23)$$

$$F_6(y, s) = \frac{1}{s-f} e^{-y\sqrt{p_r s}} \quad (3.1.24)$$

$$F_7(y, s) = \frac{1}{s} e^{-y\sqrt{p_r s}} \quad (3.1.25)$$

$$F_8(y, s) = \frac{1}{s^2} e^{-y\sqrt{p_r s}} \quad (3.1.26)$$

$$F_9(y, s) = \frac{e^{-y\sqrt{\frac{s+b}{a}}}}{s-g} \quad (3.1.27)$$

$$F_{10}(y, s) = \frac{1}{s} e^{-y\sqrt{s_c s}} \quad (3.1.28)$$

$$F_{11}(y, s) = \frac{1}{s^2} e^{-y\sqrt{s_c s}} \quad (3.1.29)$$

$$F_{12}(y, s) = \frac{1}{s-g} e^{-y\sqrt{s_c s}} \quad (3.1.30)$$

Inverse Laplace transform of equations (3.1.9) to (3.1.30),

$$\theta(y, t) = f_8(y, t) - f_8(y, t-1)H(t-1) \quad (3.1.31)$$

$$C(y, t) = f_{11}(y, t) \quad (3.1.32)$$

$$u_{sin}(y, t) = \frac{i}{2}f_1(y, t) - \frac{i}{2}f_2(y, t) + g_1(y, t) - g_1(y, t - 1)H(t - 1) - g_2(y, t) + g_2(y, t - 1) H(t - 1) + g_3(y, t) - g_4(y, t) \quad (3.1.33)$$

$$u_{cos}(y, t) = \frac{1}{2}f_1(y, t) - \frac{1}{2}f_2(y, t) + g_1(y, t) - g_1(y, t - 1)H(t - 1) - g_2(y, t) + g_2(y, t - 1) H(t - 1) + g_3(y, t) - g_4(y, t) \quad (3.1.34)$$

3.1.4.2 Solutions for Plate with Isothermal Temperature

In this case, the initial and boundary conditions are the same excluding Eq. (3.1.8) that becomes $\theta = 1$ at $y = 0, t \geq 0$. So, expression of velocity $u(y, t)$ and temperature $\theta(y, t)$ are obtained using Laplace transform technique for isothermal plates which is given below.

$$\theta(y, t) = f_7(y, t) \quad (3.1.35)$$

$$u_{sin}(y, t) = \frac{i}{2}f_1(y, t) - \frac{i}{2}f_2(y, t) + g_5(y, t) + g_3(y, t) - g_6(y, t) - g_4(y, t) \quad (3.1.36)$$

$$u_{cos}(y, t) = \frac{1}{2}f_1(y, t) + \frac{1}{2}f_2(y, t) + g_5(y, t) + g_3(y, t) - g_6(y, t) - g_4(y, t) \quad (3.1.37)$$

where

$$f_1(y, t) = \frac{e^{-i\omega_1 t}}{2} \left[e^{-y\sqrt{\frac{1}{a}(b-i\omega_1)}} \operatorname{erfc} \left(\frac{y\frac{1}{\sqrt{a}}}{2\sqrt{t}} - \sqrt{(b-i\omega_1)t} \right) + e^{y\sqrt{\frac{1}{a}(b-i\omega_1)}} \operatorname{erfc} \left(\frac{y\frac{1}{\sqrt{a}}}{2\sqrt{t}} + \sqrt{(b-i\omega_1)t} \right) \right] \quad (3.1.38)$$

$$f_2(y, t) = \frac{e^{i\omega_1 t}}{2} \left[e^{-y\sqrt{\frac{1}{a}(b+i\omega_1)}} \operatorname{erfc} \left(\frac{y\frac{1}{\sqrt{a}}}{2\sqrt{t}} - \sqrt{(b+i\omega_1)t} \right) + e^{y\sqrt{\frac{1}{a}(b+i\omega_1)}} \operatorname{erfc} \left(\frac{y\frac{1}{\sqrt{a}}}{2\sqrt{t}} + \sqrt{(b+i\omega_1)t} \right) \right] \quad (3.1.39)$$

$$g_1(y, t) = a_1 f_3(y, t) + a_2 f_4(y, t) + a_3 f_5(y, t) \quad (3.1.40)$$

$$g_2(y, t) = a_1 f_6(y, t) + a_2 f_7(y, t) + a_3 f_8(y, t) \quad (3.1.41)$$

$$g_3(y, t) = a_4 f_4(y, t) + a_5 f_5(y, t) + a_6 f_9(y, t) \quad (3.1.42)$$

$$g_4(y, t) = a_4 f_{10}(y, t) + a_5 f_{11}(y, t) + a_6 f_{12}(y, t) \quad (3.1.43)$$

$$g_5(y, t) = a_3 f_4(y, t) - a_3 f_3(y, t) \quad (3.1.44)$$

$$g_6(y, t) = a_3 f_7(y, t) - a_3 f_6(y, t) \quad (3.1.45)$$

$$f_3(y, t) = \frac{e^{ft}}{2} \left[e^{-y\sqrt{\frac{1}{a}(b+f)}} \operatorname{erfc} \left(\frac{y}{2\sqrt{at}} - \sqrt{(b+f)t} \right) + e^{y\sqrt{\frac{1}{a}(b+f)}} \operatorname{erfc} \left(\frac{y}{2\sqrt{at}} + \sqrt{(b+f)t} \right) \right] \quad (3.1.46)$$

$$f_4(y, t) = \frac{1}{2} \left[e^{-y\sqrt{\frac{b}{a}}} \operatorname{erfc} \left(\frac{y}{2\sqrt{at}} - \sqrt{bt} \right) + e^{y\sqrt{\frac{b}{a}}} \operatorname{erfc} \left(\frac{y}{2\sqrt{at}} + \sqrt{bt} \right) \right] \quad (3.1.47)$$

$$f_5(y, t) = \frac{1}{2} \left[\left(t - \frac{y}{2\sqrt{ab}} \right) e^{-y\sqrt{\frac{b}{a}}} \operatorname{erfc} \left(\frac{y}{2\sqrt{at}} - \sqrt{bt} \right) + \left(t + \frac{y}{2\sqrt{ab}} \right) e^{y\sqrt{\frac{b}{a}}} \operatorname{erfc} \left(\frac{y}{2\sqrt{at}} + \sqrt{bt} \right) \right] \quad (3.1.48)$$

$$f_6(y, t) = \frac{e^{ft}}{2} \left[e^{-y\sqrt{Prf}} \operatorname{erfc} \left(\frac{y\sqrt{Pr}}{2\sqrt{t}} - \sqrt{ft} \right) + e^{y\sqrt{Prf}} \operatorname{erfc} \left(\frac{y\sqrt{Pr}}{2\sqrt{t}} + \sqrt{ft} \right) \right] \quad (3.1.49)$$

$$f_7(y, t) = \operatorname{erfc} \left(\frac{y\sqrt{Pr}}{2\sqrt{t}} \right) \quad (3.1.50)$$

$$f_8(y, t) = \left(\frac{y^2 Pr}{2} + t \right) \operatorname{erfc} \left(\frac{y\sqrt{Pr}}{2\sqrt{t}} \right) - \frac{y\sqrt{Pr}t}{2\sqrt{\pi}} e^{-\frac{y^2 Pr}{4t}} \quad (3.1.51)$$

$$f_9(y, t) = \frac{e^{gt}}{2} \left[e^{-y\sqrt{\frac{1}{a}(b+g)}} \operatorname{erfc} \left(\frac{y}{2\sqrt{at}} - \sqrt{(b+g)t} \right) + e^{y\sqrt{\frac{1}{a}(b+g)}} \operatorname{erfc} \left(\frac{y}{2\sqrt{at}} + \sqrt{(b+g)t} \right) \right] \quad (3.1.52)$$

$$f_{10}(y, t) = \operatorname{erfc} \left(\frac{y\sqrt{Sc}}{2\sqrt{t}} \right) \quad (3.1.53)$$

$$f_{11}(y, t) = \left(\frac{y^2 Sc}{2} + t \right) \operatorname{erfc} \left(\frac{y\sqrt{Sc}}{2\sqrt{t}} \right) - \frac{y\sqrt{Sc}t}{2\sqrt{\pi}} e^{-\frac{y^2 Sc}{4t}} \quad (3.1.54)$$

$$f_{12}(y, t) = \frac{e^{gt}}{2} \left[e^{-y\sqrt{Scg}} \operatorname{erfc} \left(\frac{y\sqrt{Sc}}{2\sqrt{t}} - \sqrt{gt} \right) + e^{y\sqrt{Scg}} \operatorname{erfc} \left(\frac{y\sqrt{Sc}}{2\sqrt{t}} + \sqrt{gt} \right) \right] \quad (3.1.55)$$

Where $u_{sin}(y, t)$ and $u_{cos}(y, t)$ are the velocity profiles for sin and cosine oscillations for the ramped and isothermal temperatures respectively.

3.1.4.3 Nusselt number

The Nusselt number Nu can be written as

$$N_u = -\left(\frac{\partial\theta}{\partial y}\right)_{y=0} \quad (3.1.56)$$

Using the equation (3.1.31), it is obtained the Nusselt number for Ramped wall temperature is

$$N_u = -[h_{12}(t) - h_{12}(t-1)H(t-1)] \quad (3.1.57)$$

Using the equation (3.1.35), it is obtained the Nusselt number for Isothermal temperature is

$$N_u = -[h_{11}(t)] \quad (3.1.58)$$

3.1.4.4 Sherwood number

Sherwood number is defined and denoted by the formula

$$s_h = -\left(\frac{\partial C}{\partial y}\right)_{y=0} \quad (3.1.59)$$

Using the equation (3.1.32), it is obtained the Sherwood number is

$$s_h = -[h_{15}(t)] \quad (3.1.60)$$

3.1.4.5 Skin friction

Expressions of skin-friction for both cases are calculated from Equations (3.1.33), (3.1.34) and equations (3.1.36), (3.1.37) using the relations

$$\tau^*(y, t) = -\mu_B \left(1 + \frac{1}{\gamma}\right) \tau \quad (3.1.61)$$

$$\text{Where } \tau = \left.\frac{\partial u}{\partial y}\right|_{y=0} \quad (3.1.62)$$

For ramped wall temperature

$$\tau_{sin}(y, t) = \frac{i}{2}h_1(t) - \frac{i}{2}h_2(t) + h_3(t) - h_3(t-1)H(t-1) - h_4(t) + h_4(t-1)H(t-1) + h_5(t) - h_6(t) \quad (3.1.63)$$

$$\tau_{cos}(y, t) = \frac{1}{2}h_1(t) + \frac{1}{2}h_2(t) + h_3(t) - h_3(t-1)H(t-1) - h_4(t) + h_4(t-1)H(t-1) + h_5(t) - h_6(t) \quad (3.1.64)$$

For isothermal temperature

$$\tau_{sin}(y, t) = \frac{i}{2}h_1(t) - \frac{i}{2}h_2(t) + h_{17}(t) + h_5(t) - h_{18}(t) - h_6(t) \quad (3.1.65)$$

$$\tau_{cos}(y, t) = \frac{1}{2}h_1(t) + \frac{1}{2}h_2(t) + h_{17}(t) + h_5(t) - h_{18}(t) - h_6(t) \quad (3.1.66)$$

Where

$$h_1(t) = e^{-i\omega_1 t} \sqrt{\frac{b-i\omega_1}{a}} \operatorname{erf}(\sqrt{(b-i\omega_1)t}) + \frac{e^{-bt}}{\sqrt{\pi at}} \quad (3.1.67)$$

$$h_2(t) = e^{i\omega_1 t} \sqrt{\frac{b+i\omega_1}{a}} \operatorname{erf}(\sqrt{(b+i\omega_1)t}) + \frac{e^{-bt}}{\sqrt{\pi at}} \quad (3.1.68)$$

$$h_3(t) = a_1 h_7(t) + a_2 h_8(t) + a_3 h_9(t) \quad (3.1.69)$$

$$h_4(t) = a_1 h_{10}(t) + a_2 h_{11}(t) + a_3 h_{12}(t) \quad (3.1.70)$$

$$h_5(t) = a_4 h_8(t) + a_5 h_9(t) + a_6 h_{13}(t) \quad (3.1.71)$$

$$h_6(t) = a_4 h_{14}(t) + a_5 h_{15}(t) + a_6 h_{16}(t) \quad (3.1.72)$$

$$h_7(t) = e^{ft} \sqrt{\frac{b+f}{a}} \operatorname{erf}(\sqrt{(b+f)t}) + \frac{e^{-bt}}{\sqrt{\pi at}} \quad (3.1.73)$$

$$h_8(t) = -\sqrt{\frac{b}{a}} \operatorname{erf}(\sqrt{bt}) + \frac{e^{-bt}}{\sqrt{\pi at}} \quad (3.1.74)$$

$$h_9(t) = -\frac{1}{\sqrt{4ab}} \operatorname{erf}(\sqrt{bt}) - t \sqrt{\frac{b}{a}} \operatorname{erf}(\sqrt{bt}) + \sqrt{\frac{t}{\pi a}} e^{-bt} \quad (3.1.75)$$

$$h_{10}(t) = -e^{ft} \sqrt{Prf} \operatorname{erf}(\sqrt{ft}) + \sqrt{\frac{Pr}{\pi t}} \quad (3.1.76)$$

$$h_{11}(t) = \sqrt{\frac{Pr}{\pi t}} \quad (3.1.77)$$

$$h_{12}(t) = \frac{1}{2} \sqrt{\frac{tPr}{\pi}} \quad (3.1.78)$$

$$h_{13}(t) = e^{gt} \sqrt{\frac{b+g}{a}} \operatorname{erf}(\sqrt{(b+g)t}) + \frac{e^{-bt}}{\sqrt{\pi at}} \quad (3.1.79)$$

$$h_{14}(t) = \sqrt{\frac{Sc}{\pi t}} \tag{3.1.80}$$

$$h_{15}(t) = \frac{1}{2} \sqrt{\frac{tSc}{\pi}} \tag{3.1.81}$$

$$h_{16}(t) = -e^{gt} \sqrt{Scg} \operatorname{erf}(\sqrt{gt}) + \sqrt{\frac{Sc}{\pi t}} \tag{3.1.82}$$

3.1.5 Results and Discussion

The non-dimensional fluid velocity, temperature and concentration profiles for several values of Prandtl number Pr , thermal Grashof number Gr , mass Grashof number Gm , Casson fluid parameter γ , magnetic parameter M , permeability of porous medium k , phase angle ω_1 and time t are presented in Figures (3.1.2) to Figures (3.1.13). Figure 3.1.2 shows velocity decreased with increase in γ for $\omega_1 = \frac{\pi}{2}$ whereas, velocity increased with increase in γ for $\omega_1 = 0$. It is also seen that, when the Casson parameter γ is large enough, the non-Newtonian behaviours disappear and the fluid purely behaves like a Newtonian fluid. Thus, the velocity boundary layer thickness for Casson fluid is larger than the Newtonian fluid. It occurs because of plasticity of Casson fluid.

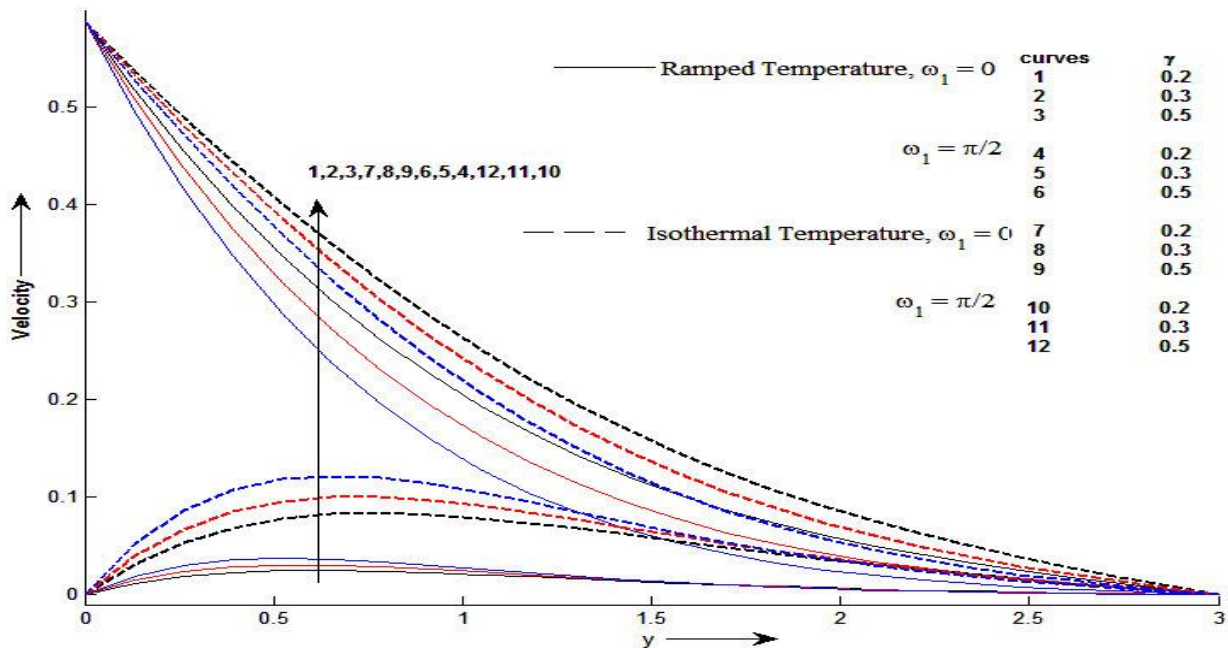


Figure 3.1.2: Velocity profile u for different values of y and γ at $M = 0.5, Sc = 1, Gm = 2, Gr = 3, k = 0.2, t = 0.4$ and $Pr = 0.7$.

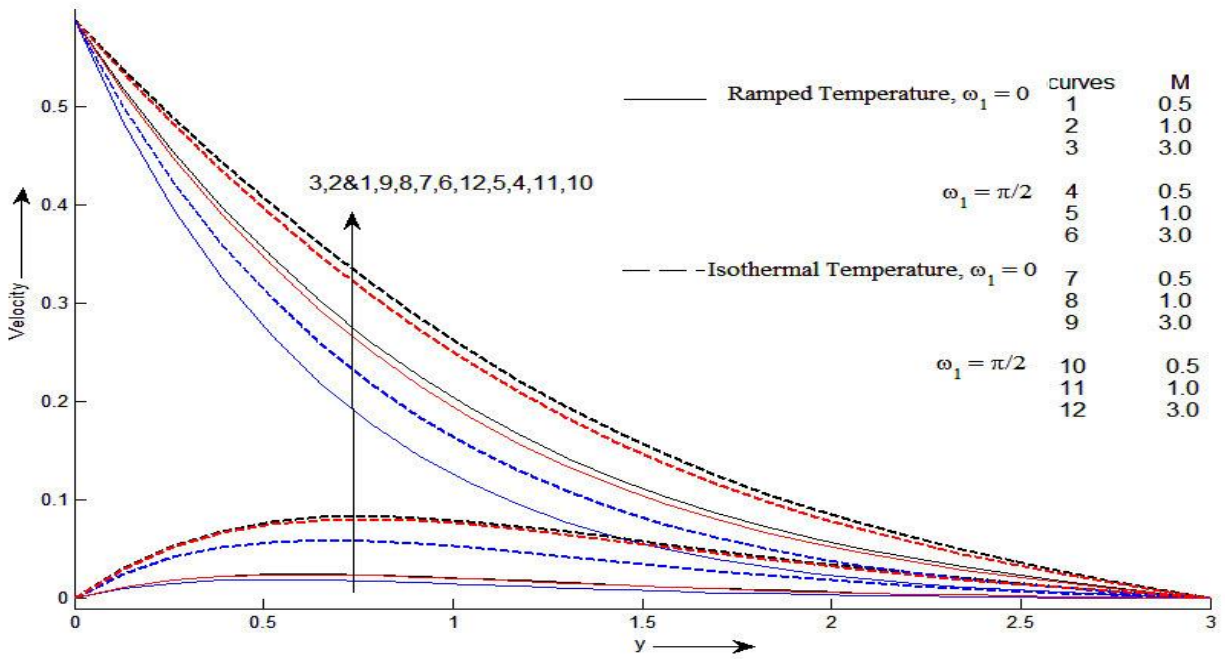


Figure 3.1.3: Velocity profile u for different values of y and M , at $Pr = 0.7, Sc = 1, Gm = 2, Gr = 3, k = 0.2, t = 0.4$ and $\gamma = 0.6$.

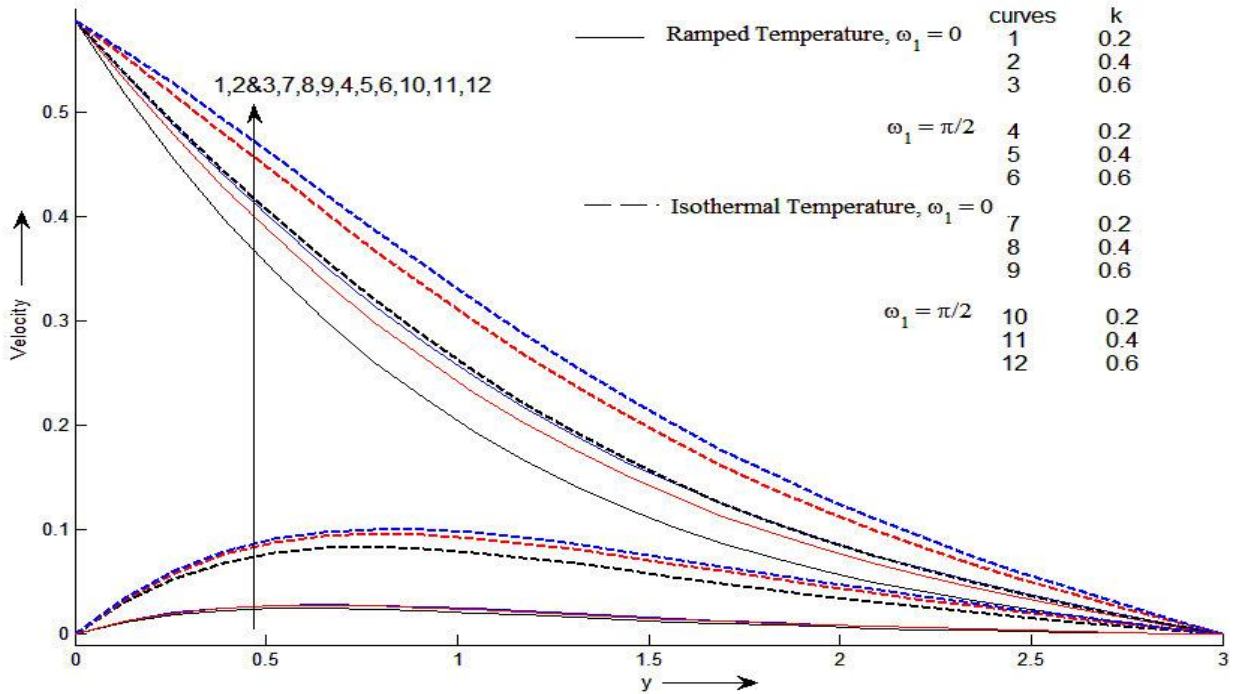


Figure 3.1.4: Velocity profile u for different values of y and k at $Pr = 7, Sc = 1, Gm = 2, Gr = 3, t = 0.4$ and $\gamma = 0.2$.

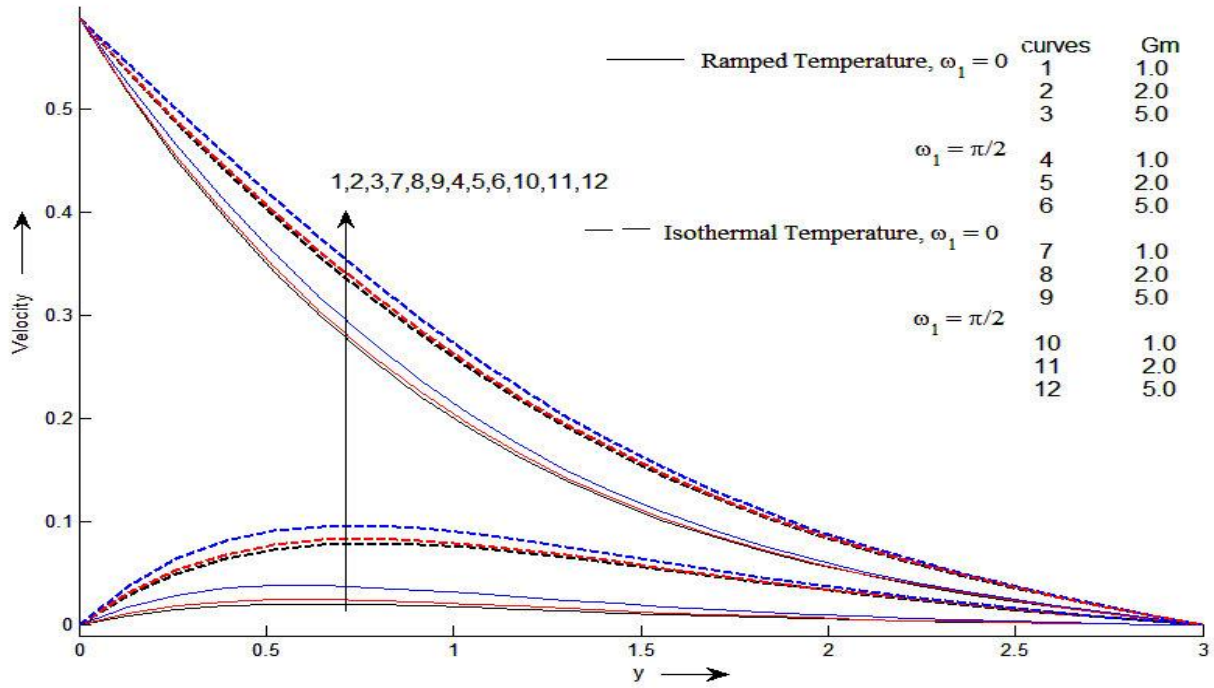


Figure 3.1.5: Velocity profile u for different values of y and Gm at $Pr = 0.7, Sc = 1, Gr = 3, k = 0.2, t = 0.4, M = 0.5$ and $\gamma = 0.2$.

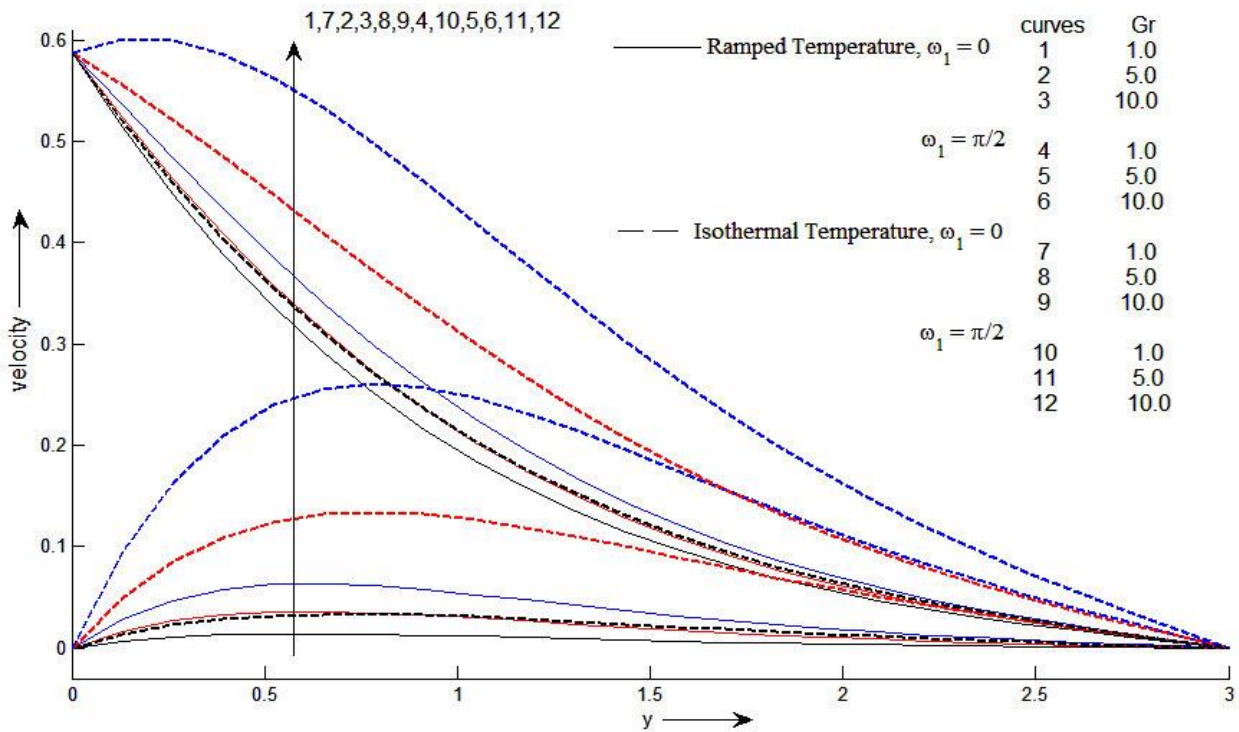


Figure 3.1.6: Velocity profile u for different values of y and Gr at $Pr = 0.7, Sc = 1, Gr = 3, k = 0.2, t = 0.4$ and $\gamma = 0.2$.

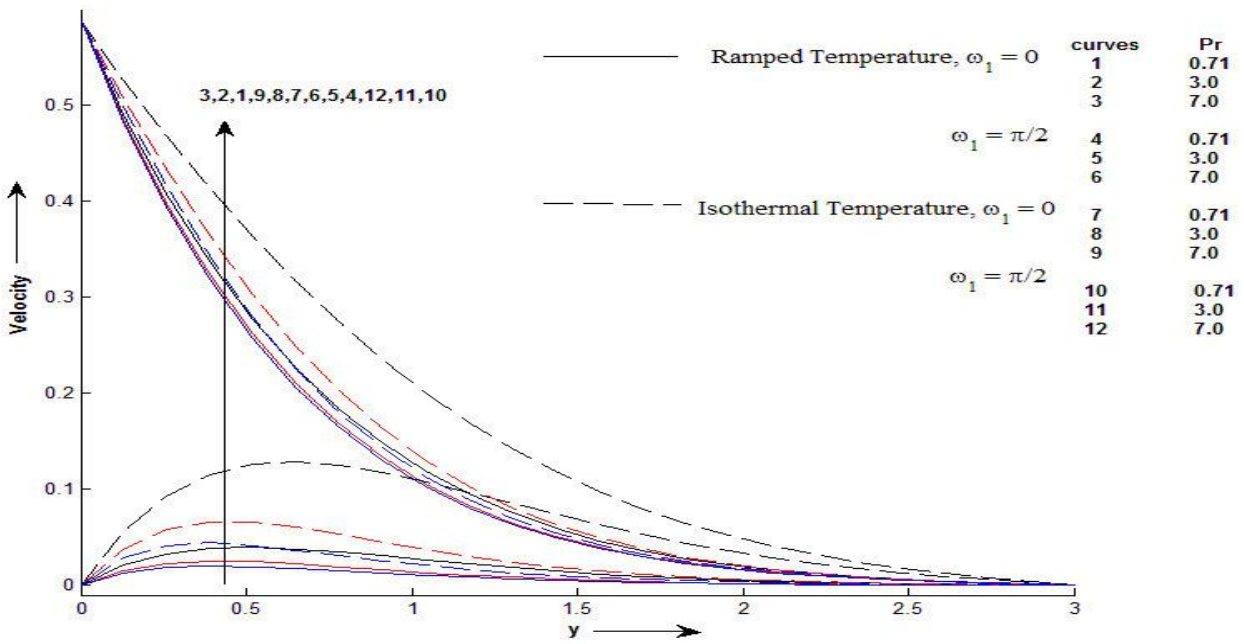


Figure 3.1.7: Velocity profile u for different values of y and Pr at $M = 0.5, Sc = 1, Gm = 2, Gr = 3, k = 0.2, t = 0.4$ and $\gamma = 0.6$.

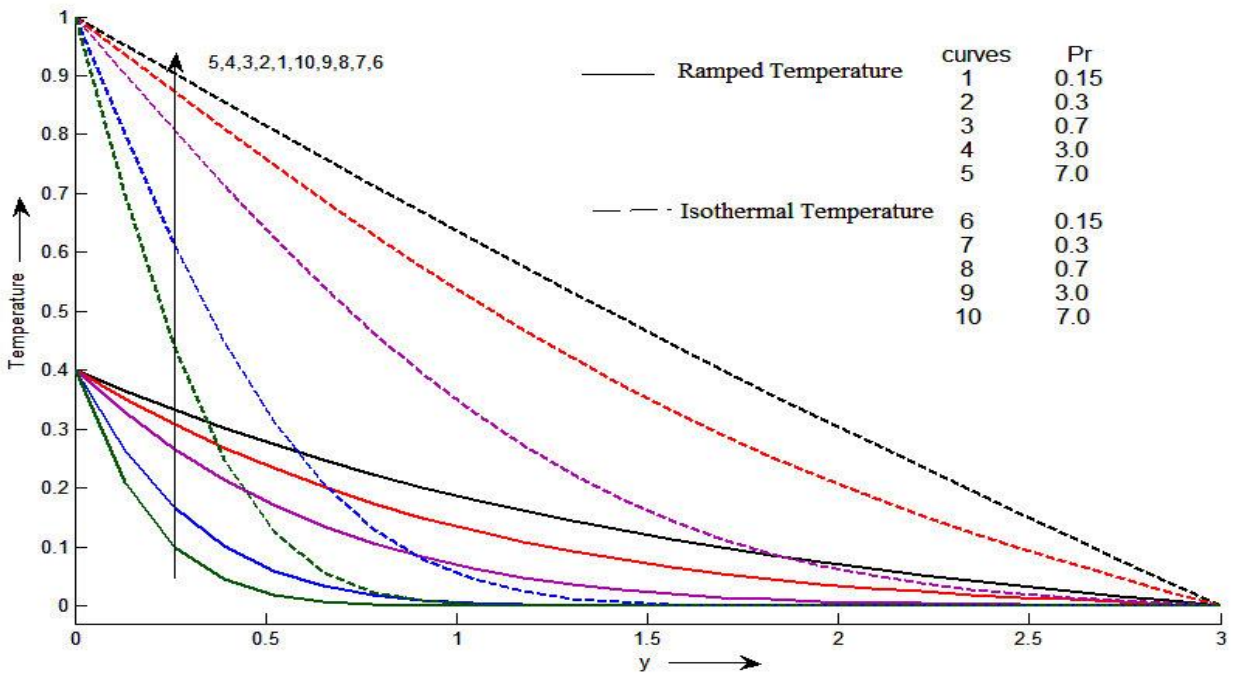


Figure 3.1.8: Temperature profile θ for different values of y and Pr at $t = 0.4$

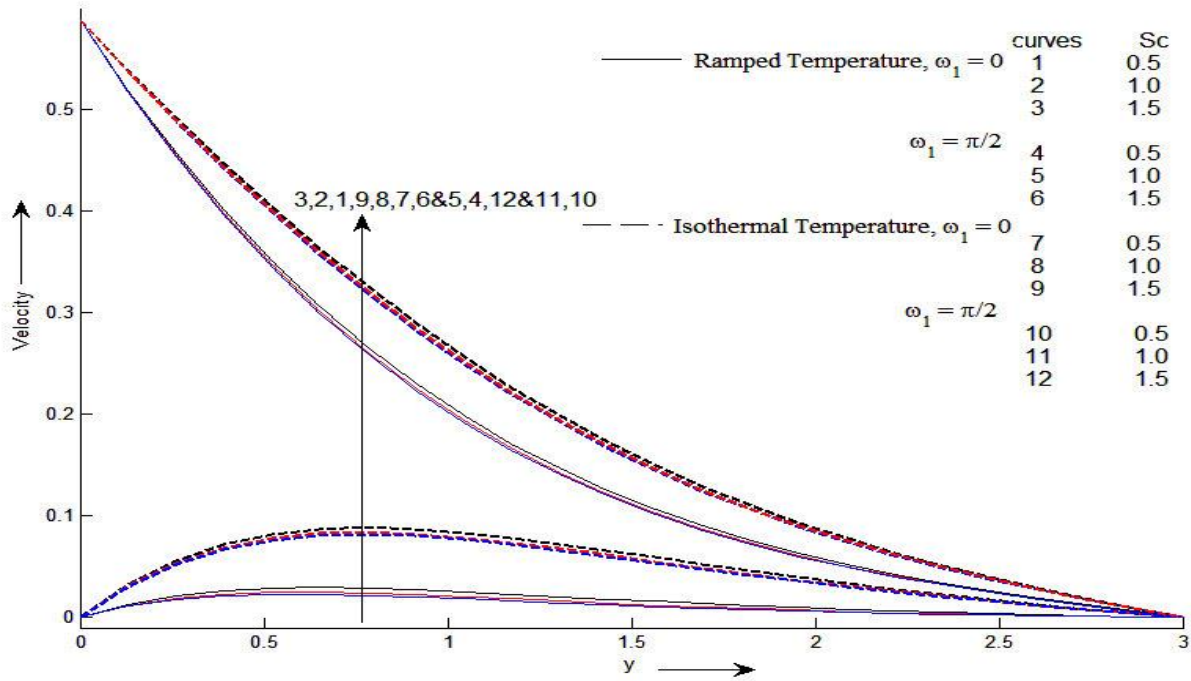


Figure 3.1.9: Velocity profile u for different values of y and Sc at $Pr = 0.7$, $Gm = 2$, $Gr = 3$, $k = 0.2$, $t = 0.4$, $M = 0.5$ and $\gamma = 0.6$.

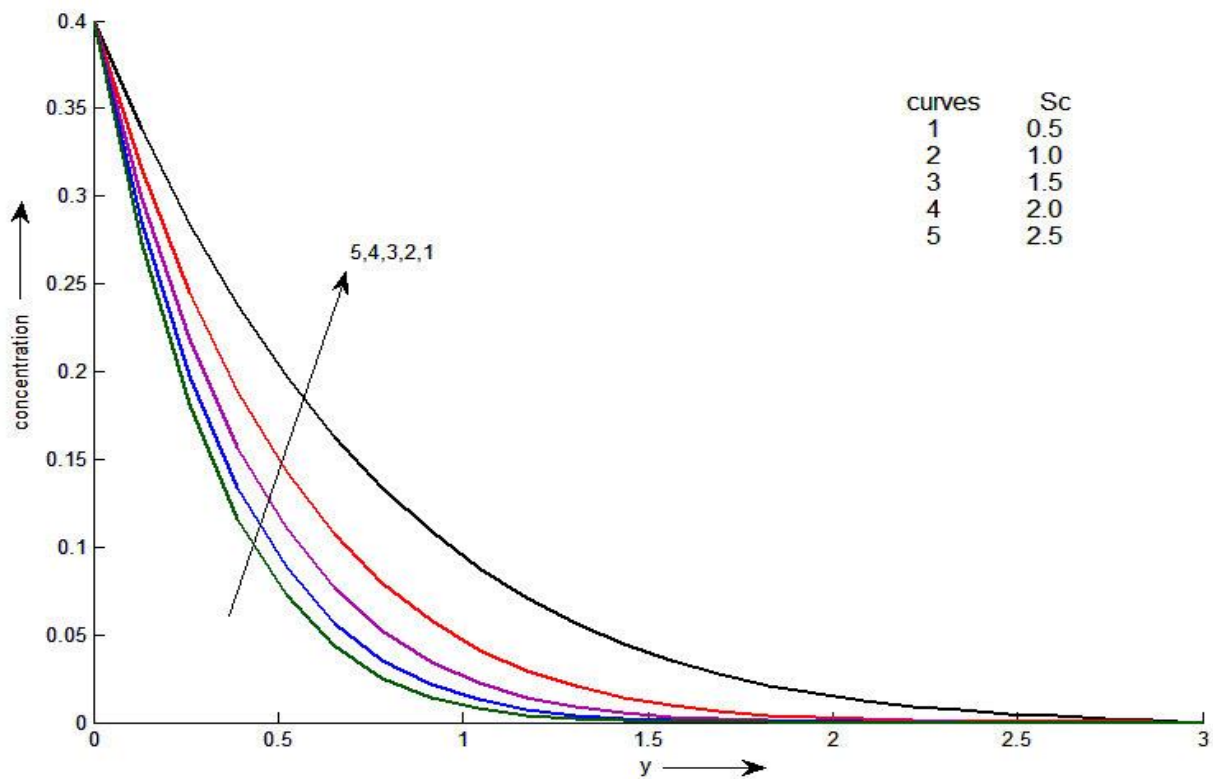


Figure 3.1.10: Concentration profile C for different values of y and Sc at $t = 0.4$

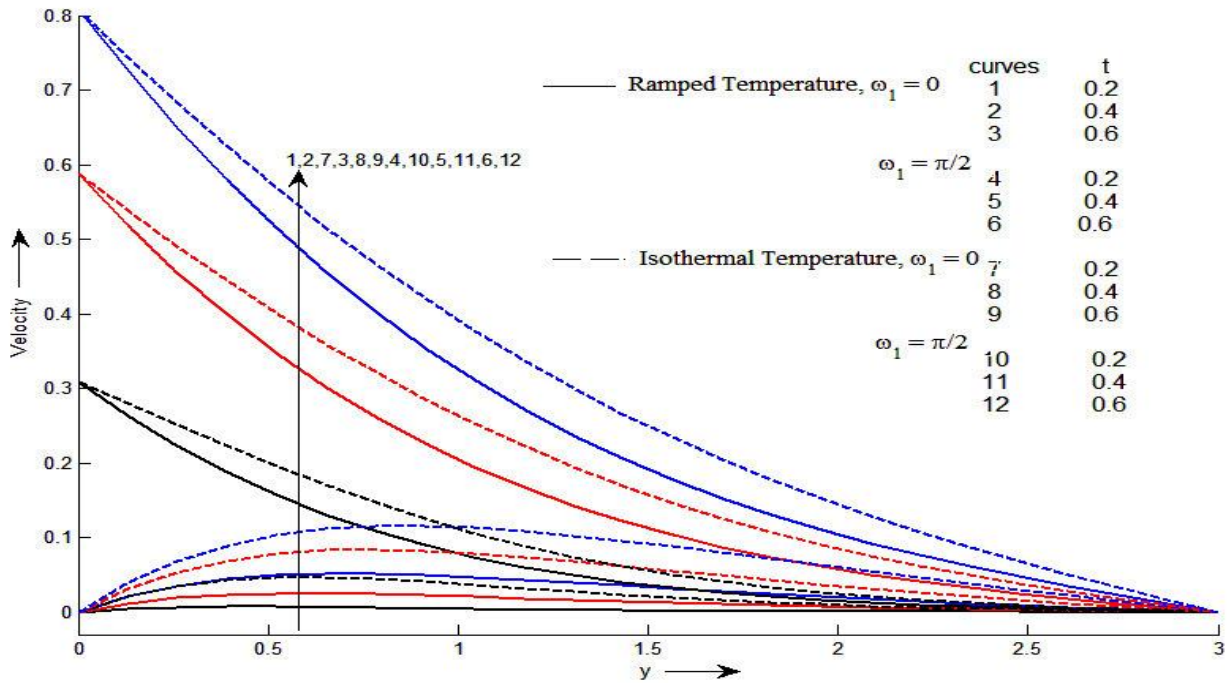


Figure 3.1.11: Velocity profile u for different values of y and t at $M = 0.5, Pr = 0.7, Sc = 1, Gr = 3, Gm = 2, k = 0.2, t = 0.4$ and $\gamma = 0.2$.

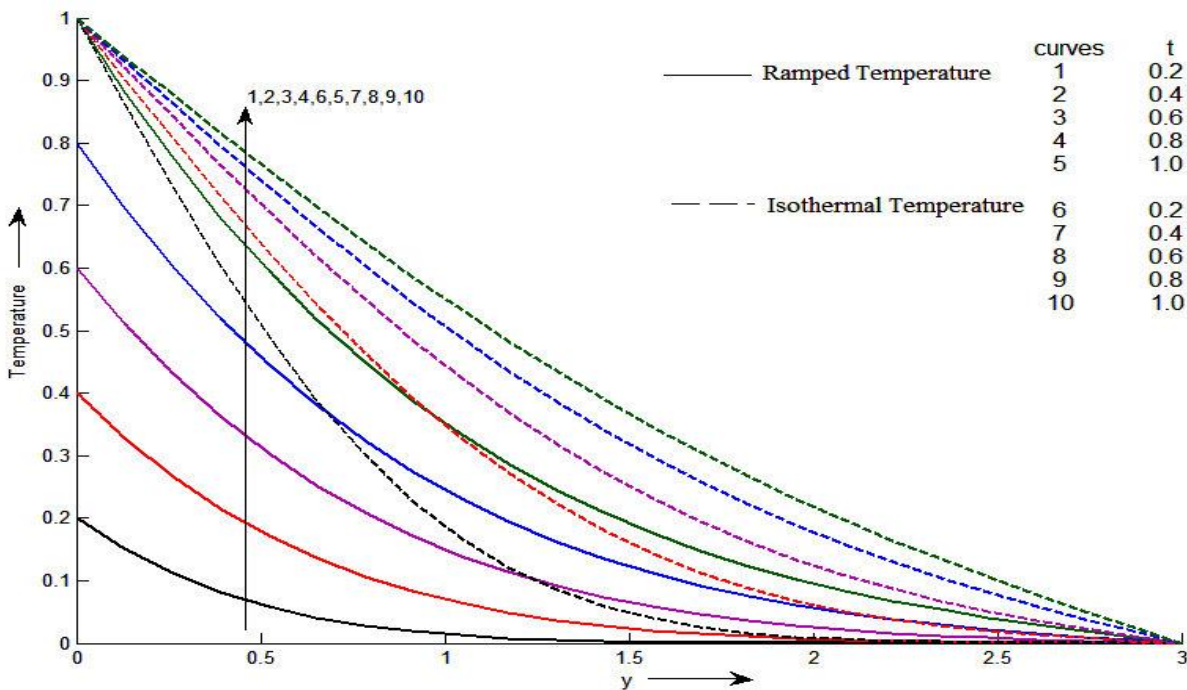


Figure 3.1.12: Temperature profile θ for different values of y and t at $Pr = 0.7$

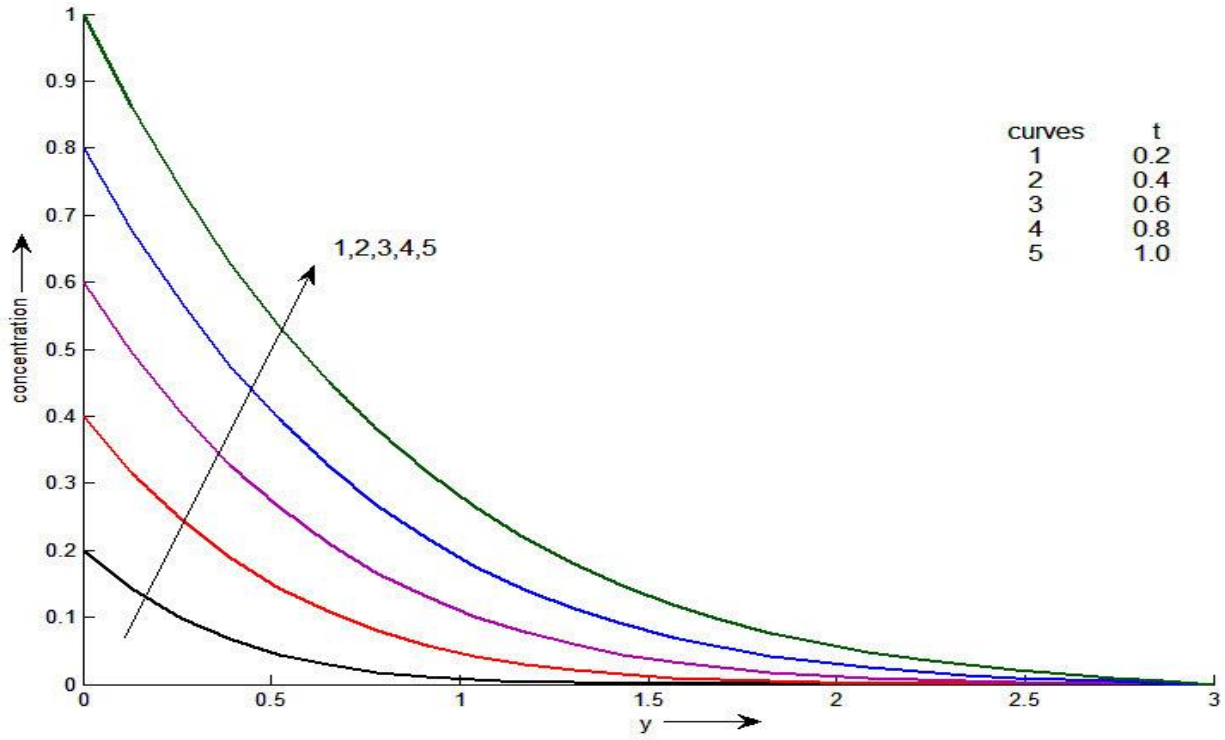


Figure 3.1.13: Concentration profile C for different values of y and t at $Sc = 1$

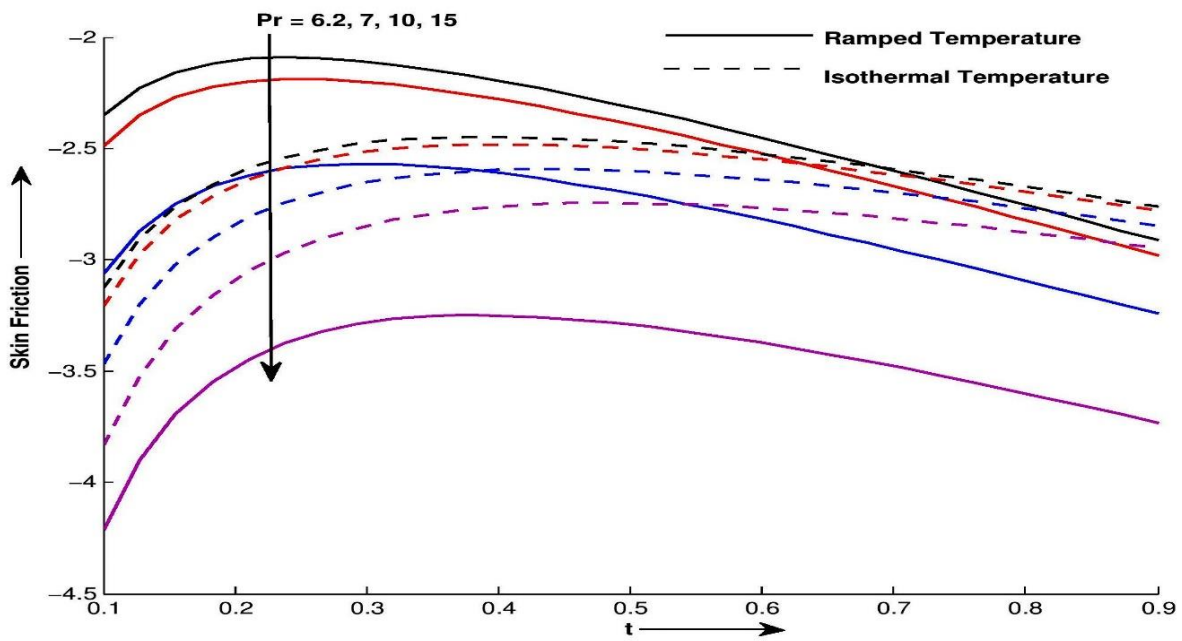


Figure 3.1.14: Skin friction τ for different values of t and Pr at $k = 1, \gamma = 1, M = 5,$
 $Sc = 6.2, Gr = 2$ and $Gm = 5$

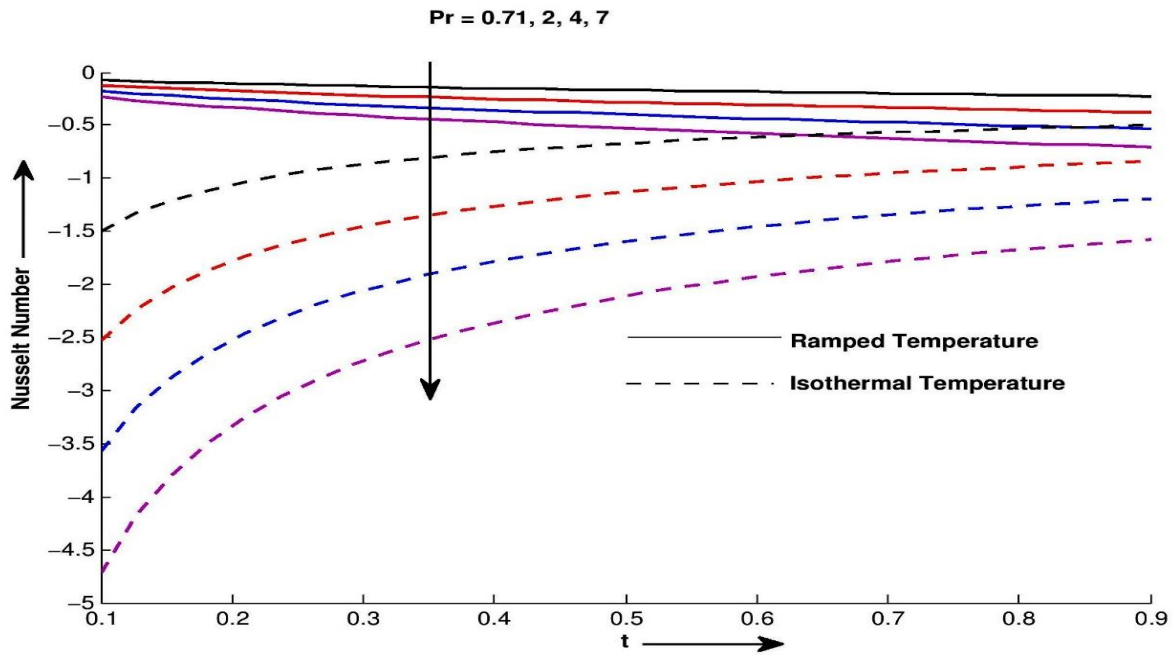


Figure 3.1.15: Nusselt number Nu for different values of t and Pr .

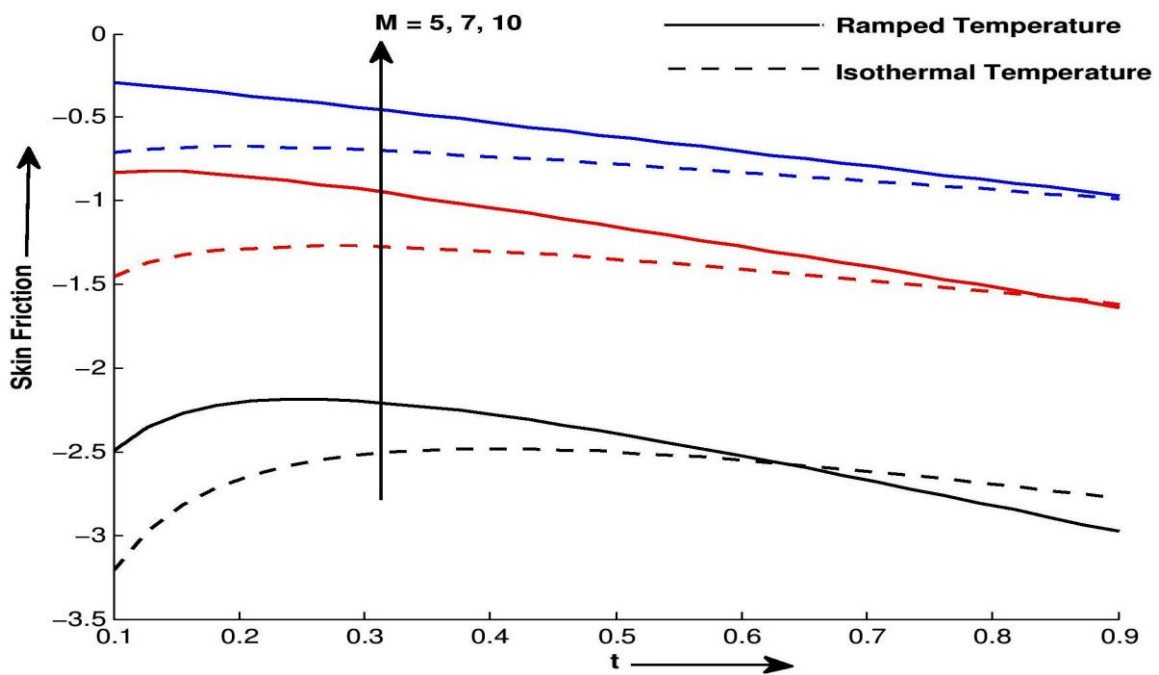


Figure 3.1.16: Skin friction τ for different values of t and M at $k = 1, \gamma = 1, Pr = 7, Sc = 6.2, Gr = 2$ and $Gm = 5$.

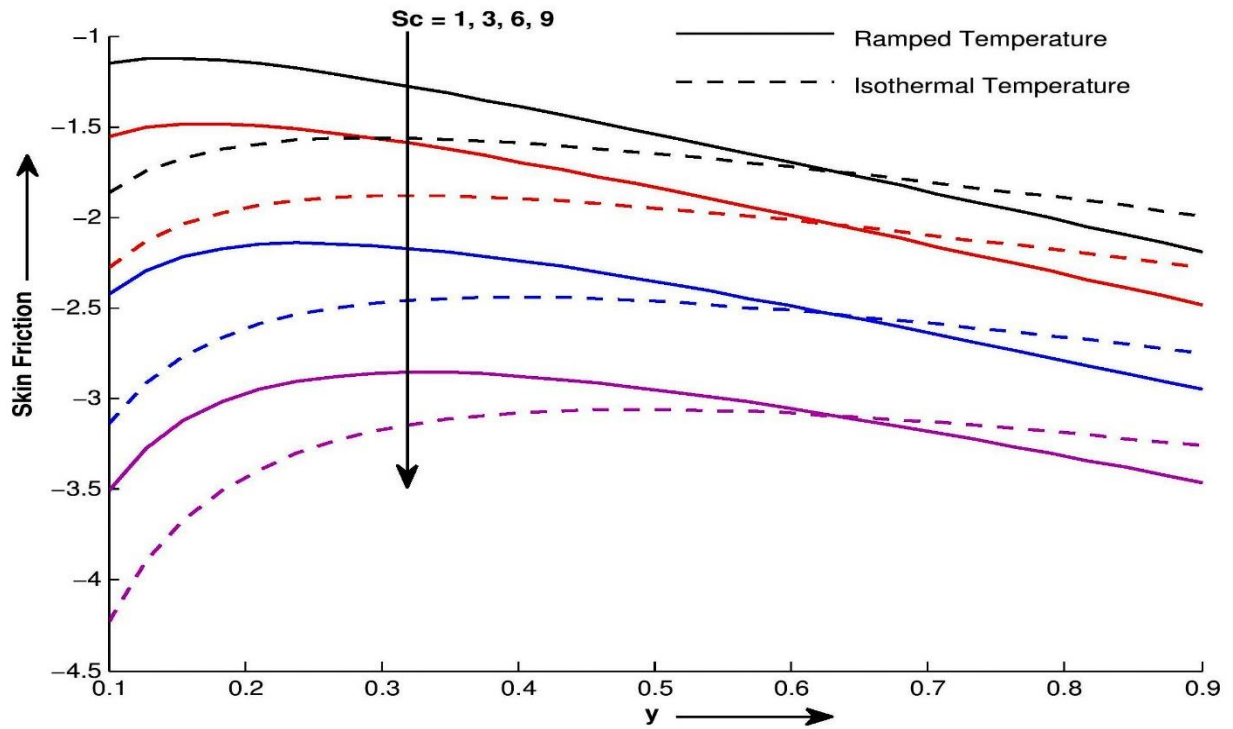


Figure 3.1.17: Skin friction τ for different values of t and Sc at $k = 1, \gamma = 1, Pr = 7, M = 5, Gr = 2$ and $Gm = 5$.

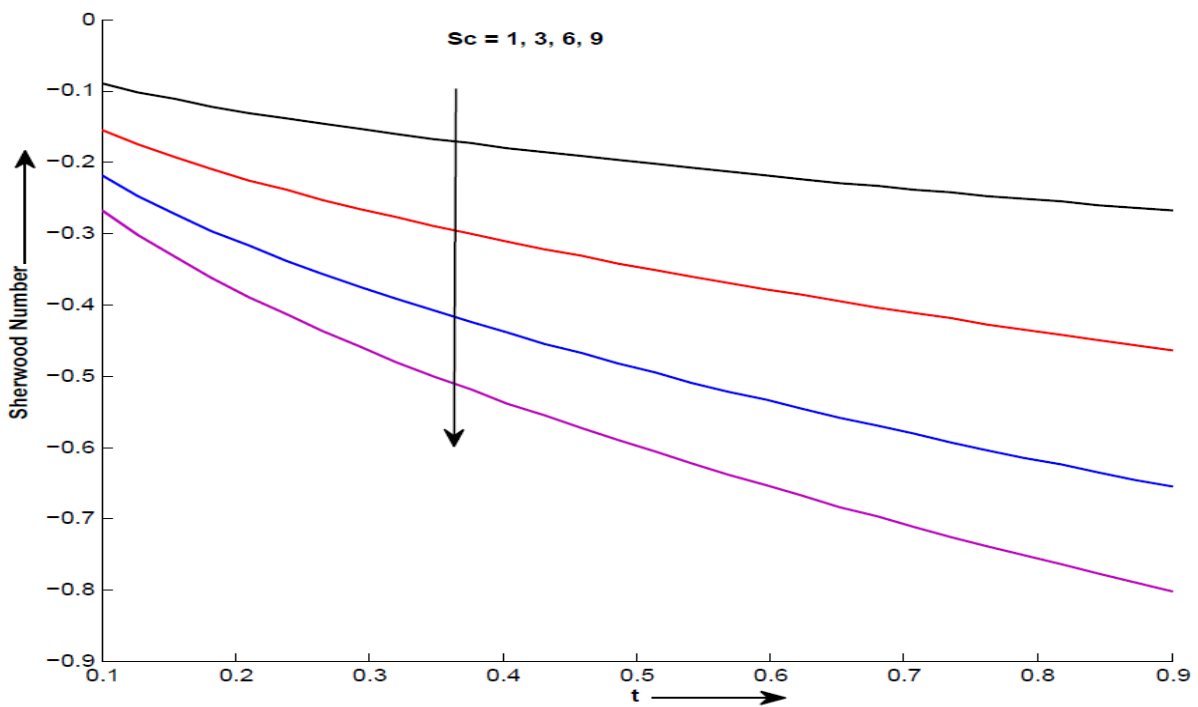


Figure 3.1.18: Sherwood number Sh for different values of t and Sc .

Table 3.1.1: Skin friction variation for air ($Pr = 0.71$ and $Sin \omega_1 t = 0$)

t	γ	Sc	Gr	Gm	M	k	Skin friction τ for Ramped Temperature	Skin friction τ for Isothermal Temperature
0.4	1	0.6	2	4	2	1	-2.5439	-3.5534
0.4	1.1	0.6	2	4	2	1	-2.4115	-3.4060
0.4	1.2	0.6	2	4	2	1	-2.3037	-3.2843
0.4	1	0.7	2	4	2	1	-2.7201	-3.7297
0.4	1	0.8	2	4	2	1	-2.9049	-3.9144
0.4	1	0.6	2.5	4	2	1	-2.7720	-4.0340
0.4	1	0.6	3.0	4	2	1	-3.0002	-4.5146
0.4	1	0.6	2	4.5	2	1	-2.7478	-3.7573
0.4	1	0.6	2	5.0	2	1	-2.9516	-3.9612
0.4	1	0.6	2	4	2.2	1	-2.2335	-3.1650
0.4	1	0.6	2	4	2.5	1	-1.8788	-2.7088
0.4	1	0.6	2	4	2	1.1	-2.4967	-3.4950
0.4	1	0.6	2	4	2	1.2	-2.4406	-3.4252
0.5	1	0.6	2	4	2	1	-2.9537	-3.7489
0.6	1	0.6	2	4	2	1	-3.3619	-3.9658

Table 3.1.2: Skin friction variation for water ($Pr = 7$ and $Sin \omega_1 t = 0$)

t	γ	Sc	Gr	Gm	M	k	Skin friction τ for Ramped temperature	Skin friction τ for isothermal temperature
0.4	1	0.6	2	4	2	1	-13.4431	-5.7863
0.4	1.1	0.6	2	4	2	1	-12.3686	-5.5290
0.4	1.2	0.6	2	4	2	1	-11.5080	-5.3159
0.4	1	0.7	2	4	2	1	-13.6194	-5.9625
0.4	1	0.8	2	4	2	1	-13.8041	-6.1473
0.4	1	0.6	2.5	4	2	1	-16.3961	-6.8250
0.4	1	0.6	3.0	4	2	1	-19.3491	-7.8638
0.4	1	0.6	2	4.5	2	1	-13.6470	-5.9901
0.4	1	0.6	2	5.0	2	1	-13.8509	-6.1940
0.4	1	0.6	2	4	2.2	1	-10.3567	-5.0447
0.4	1	0.6	2	4	2.5	1	-7.2917	-4.1850
0.4	1	0.6	2	4	2	1.1	-12.9505	-5.6742

0.4	1	0.6	2	4	2	1.2	-12.3762	-5.5408
0.5	1	0.6	2	4	2	1	-12.9441	-5.6975
0.6	1	0.6	2	4	2	1	-12.6967	-5.7063

Table 3.1.3: Nusselt number variation for air ($Pr = 0.71$)

t	Nusselt number Nu for Ramped Temperature	Nusselt number Nu for isothermal Temperature
0.4	-0.1503	-0.7517
0.5	-0.1681	-0.6723
0.6	-0.1841	-0.6137
0.7	-0.1989	-0.5682

Table 3.1.4: Nusselt number variation for water ($Pr = 7$)

t	Nusselt number Nu for Ramped Temperature	Nusselt number Nu for isothermal Temperature
0.4	-0.4720	-2.3602
0.5	-0.5278	-2.1110
0.6	-0.5781	-1.9271
0.7	-0.6244	-1.7841

Table 3.1.5: Sherwood number variation

t	Sc	Sherwood number Sh
0.4	0.6	-0.1382
0.5	0.6	-0.1545
0.6	0.6	-0.1693
0.4	0.7	-0.1493
0.4	0.8	-0.1596

Figure 3.1.3 displays the effect of magnetic parameter M on the velocity profiles. It is observed that the fluid velocity as well as the boundary layer thickness decreases when M is increased. Physically, the drag force increases which leads to the slowing of the flow. Figure 3.1.4 illustrates velocity profile for various values of permeability parameter k by keeping other parameters fixed. It is seen that for increasing values of k , the resistance of the porous medium is lowered which increases the momentum development of the flow regime. The thermal Grashof number Gr indicates the ratio of thermal buoyancy force to viscous hydrodynamic force and mass Grashof number Gm point out the ratio of mass buoyancy force to viscous hydrodynamic force. It is seen that, thermal and mass

Grashof number tends to improved motion of the flow field throughout the boundary layer in Figure 3.1.5 and Figure 3.1.6 respectively. This implies that motion of fluid accelerated due to improvement in either temperature buoyancy force or mass buoyancy force. Figure 3.1.7 and Figure 3.1.8 exhibits the velocity and temperature profiles for different values of Prandtl number Pr . It is observed that momentum and heat transfer process decreases with increase in Prandtl number Pr . It is justified due to the fact that thermal conductivity of the fluid decrease with increase in Prandtl number Pr and hence decrease the thermal boundary layer thickness. The graphical results for Sc is shown in Figure 3.1.9 and Figure 3.1.10. It is depict that the fluid velocity and concentration decreases with increase in Sc . Figure 3.1.11 to Figure 3.1.13 shows the influence of dimensionless time t on the velocity, temperature and concentration profiles. It is found that the velocity, temperature and concentration profiles increases with time t . Figure 3.1.14 and Figure 3.1.15 shows effect of Pr on Skin friction and Nusselt number. For both thermal plates, Prandtl Number Pr tends to reduced Skin friction and Nusselt number variation. Physically, when fluid attains a higher Prandtl number, its thermal conductivity is decreased and so its heat conduction capacity diminishes. Thus the thermal boundary layer thickness is reduced. As a results, the heat transfer rate at the plate is reduced as Prandtl number increases. Figure 3.1.16 shows effect of magnetic field M on Skin friction. It is evident that Skin friction increase with increase in M . Figure 3.1.17 and Figure 3.1.18 illustrate that effect of Schmidt Number Sc on Skin friction and Sherwood number. From these figures it is concluded that Skin friction and Sherwood number variation decreases with increases in Sc .

The variation of the Skin friction and Nusselt number for air ($Pr = 0.71$) and water ($Pr = 7$) are shown in Tables (3.1.1) to Tables (3.1.4) for various values of the governing parameters. The increased shear stress is generally a disadvantage in applications. The negative value of Skin friction means that the plate exerts a drag force on the fluid (and vice versa). For both thermal cases, Skin friction increases with increase in γ and M , while Skin friction decreases with increase in Sc , Gr , Gm , k and t . Since the positive buoyancy force acts like a favourable pressure gradient, the fluid in the boundary layer is accelerated. Accordingly, the hot fluid near the plate surface is carried away more quickly as Grashof number Gr increases. Therefore, the shear stress at the plate reduces. From Table (3.1.3) and Table (3.1.4), it is observed that, for ramped wall temperature time variable t tends to reduced Nusselt number, while for isothermal plate time variable t tends to reverse effect on it. From Table (3.1.5), it is conclude that Sherwood number decrease with increase in t and Sc . For all governing parameter for air, magnitude of Skin friction is more for isothermal temperature

compared to ramped wall temperature but in water, magnitude of Skin friction is more for ramped temperature compared to isothermal temperature. In both physical quantities air and water, Magnitude of Nusselt number is more for ramped wall temperature compared to isothermal temperature.

3.1.6 Concluding Remark

The most significant concluding explanations can be brief as follows:

- Velocity of the fluid decreased with increase in magnetic field M , Prandtl number Pr and Schmidt number Sc throughout the flow field.
- Velocity decreased with increasing values of Casson parameter γ for $\omega_1 = \frac{\pi}{2}$ whereas increased with increasing value of γ for $\omega_1 = 0$.
- Permeability parameter k , Grashof number Gm and Gr and time variable t tends to improve motion in flow field region.
- Prandtl number Pr tends reduced heat transfer process, while time variable t tends to reverse effect on it.
- Concentration increased with increase in t , whereas decreased with increase in Sc .
- Skin friction increased with increase in γ and M , decreased with increase in Sc, Gr, Gm, k and t .
- Nusselt number is decreased with Pr and t .
- Sherwood number is decreased with Sc and t .

3.2 SECTION II: HEAT AND MASS TRANSFER EFFECTS ON MHD SECOND GRADE FLUID FLOW WITH RAMPED WALL TEMPERATURE IN POROUS MEDIUM

In this section, the unsteady MHD Second grade fluid flow past an infinite vertical plate in porous medium with ramped temperature is considered. Using some dimensionless quantities, the governing non-dimensionalized equations are converted in system of linear partial differential equation with imposed initial and boundary conditions. To analyze effect of ramped boundary condition, it is considered isothermal plate for said problem. So, for both thermal plate, expression of velocity, temperature and concentration profiles is obtained using Laplace transform technique and expression for Skin friction, Nusselt number and Sherwood number are derived. It is obtained numerical values of velocity, temperature and concentration profiles and clarified with the help of graphical illustrations.

3.2.1 Introduction of the problem

The Second grade fluids can model many fluids such as dilute polymer solutions, slurry flows and industrial oils. Tan and Masuoka [26] deliberated on stokes' first problem for a Second grade fluid while Hayat et al. [28] studied stagnation point flow of Second grade fluid.

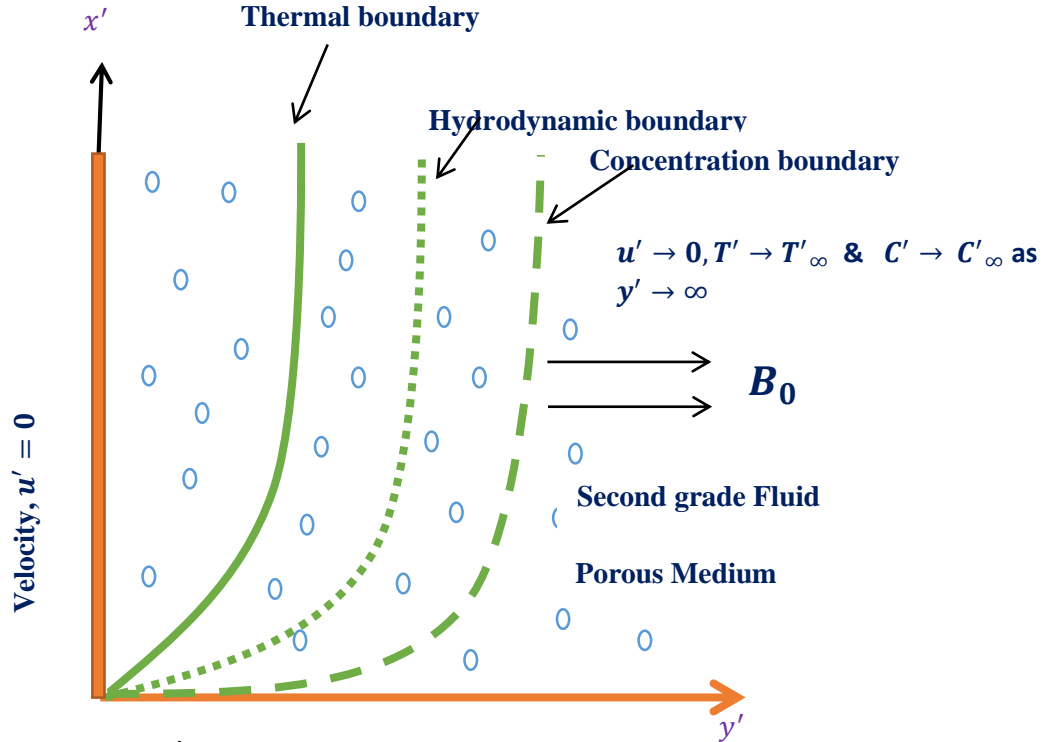
The problems of magneto hydrodynamic natural convective unsteady flow in a porous medium have drawn considerable attentions of several researchers in various scientific and technological applications. Recently, Hayat et al. [82] solved MHD flow of a Second grade fluid in a porous channel. Olanrewaju and Abbas [128] studied heat and mass transfer effects on Second grade fluid with thermal radiation and diffusion. However, in all the surveys carried out by investigators considering ramped profiles, it is to be noted that interval for ramped profile varies from material to material depending upon the specific heat capacity of the material. Khan et al. [153] defined exact solution of MHD Second grade flow of inclined vertical plate with ramped wall temperature.

3.2.2 Novelty of the problem

In previous, unsteady MHD flow of a Second grade fluid in a porous medium is studied in absence of concentration and ramped boundary condition. Therefore, study can be considered as extension of Samiulhaq et al. [155]. So, Novelty of this investigation to analyze the important role of

concentration and ramped boundary condition in MHD flow of a Second grade fluid near infinite vertical flat plate through porous medium. Finally, an analytic solution of these problem using Laplace transform technique is obtained which are shown in subsequent study.

3.2.3 Mathematical Formulation of the Problem:



$$T' = \begin{cases} T'_\infty + (T'_w - T'_\infty) t'/t_0 & \text{if } 0 < t' < t_0 \\ T'_w & \text{if } t' \geq t_0 \end{cases} \quad \& \quad C' = C'_\infty + (C'_w - C'_\infty) t'/t_0 \quad \text{as } t' > 0 \text{ and } y' = 0$$

Figure 3.2.1: Physical sketch of the problem.

In Figure 3.2.1, coordinate system is chosen such that x' – axis taken along the wall in the upward direction and y' – axis is taken normal to it. A uniformly distributed transverse magnetic field of strength B_0 is applied in the y' – axis direction. Initially, at time $t' \leq 0$, both the fluid and the plate are at constant temperature T'_∞ . The surface concentration near the plate is assumed to be C'_∞ . At the time $t' > 0$, temperature of the wall is raised or lowered to $T'_\infty + (T'_w + T'_\infty) t'/t_0$ when $t' \leq t_0$ and T'_w when $t' > t_0$ respectively which is there after maintained constant T'_w . The concentration at the surface is raised linearly to $C'_\infty + (C'_w - C'_\infty) t'/t_0$ which is there after kept constant C'_w .

It is assumed that the effects of induce magnetic field, electrical field and viscous dissipation in energy equation are neglected. It is assumed that flow is incompressible, laminar, uni-direction, one dimensional. Moreover, the plate being considered infinite in the x' -direction, all physical variables is independent of x' . Hence, the physical variables are functions of y' and t' only. One of the body force terms corresponding to MHD flow is the Lorentz force $J \times B = \sigma B_0^2 u$ as mentioned by Hayat et al. [82], where B is the total magnetic field, J is the current density, σ is electrical conductivity of the fluid and u is the velocity vector field. Under above assumptions and taking into account the Boussinesq's approximation, governing equations are given below.

$$\frac{\partial u'}{\partial t'} = \left(\nu + \frac{\alpha_1}{\rho} \frac{\partial}{\partial t'} \right) \frac{\partial^2 u'}{\partial y'^2} + g\beta'_T (T' - T'_\infty) - \frac{\sigma B_0^2}{\rho} u' - \frac{\phi}{k'} \left(\nu + \frac{\alpha_1}{\rho} \frac{\partial}{\partial t'} \right) u' + g\beta'_C (C' - C'_\infty) \quad (3.2.1)$$

$$\frac{\partial T'}{\partial t'} = \frac{k_4}{\rho c_p} \frac{\partial^2 T'}{\partial y'^2} \quad (3.2.2)$$

$$\frac{\partial C'}{\partial t'} = D_M \frac{\partial^2 C'}{\partial y'^2} \quad (3.2.3)$$

with following initial and boundary conditions

$$u' = 0, \quad T' = T'_\infty, \quad C' = C'_\infty; \text{ as } y' \geq 0 \text{ and } t' \leq 0$$

$$u' = 0, \quad T' = \begin{cases} T'_\infty + (T'_w - T'_\infty) t'/t_0 & \text{if } 0 < t' \leq t_0 \\ T'_w & \text{if } t' > t_0 \end{cases}, \quad C' = C'_\infty + (C'_w - C'_\infty); \text{ as } t' > 0 \text{ and } y' = 0$$

$$u' \rightarrow 0, T' \rightarrow T'_\infty, \quad C' \rightarrow C'_\infty; \text{ as } y' \rightarrow \infty \text{ and } t' \geq 0 \quad (3.2.4)$$

Introducing the following dimensionless quantities:

$$y = \frac{y'}{U_0 t_0}, \quad u = \frac{u'}{U_0}, \quad t = \frac{t'}{t_0}, \quad \theta = \frac{(T' - T'_\infty)}{(T'_w - T'_\infty)}, \quad C = \frac{(C' - C'_\infty)}{(C'_w - C'_\infty)}, \quad Gr = \frac{\nu g \beta'_T (T'_w - T'_\infty)}{U_0^3}$$

$$Gm = \frac{\nu g \beta'_C (C'_w - C'_\infty)}{U_0^3}, \quad M = \frac{\sigma B_0^2 \nu}{\rho U_0^2}, \quad Pr = \frac{\rho \nu c_p}{k_4}, \quad Sc = \frac{\nu}{D_M}, \quad \alpha = \frac{\alpha_1}{\rho}, \quad c = 1 + \frac{\alpha}{k'}, \quad b = M^2 + \frac{1}{k'}$$

In the equations (3.1.1 to 3.1.4) dropping out the " ' " notation (for simplicity),

$$\frac{\partial^2 u}{\partial y^2} + \alpha \frac{\partial^3 u}{\partial y^2 \partial t} - c \frac{\partial u}{\partial t} - bu + Gr\theta + Gm C = 0 \quad (3.2.5)$$

$$\frac{\partial \theta}{\partial t} = \frac{1}{Pr} \frac{\partial^2 \theta}{\partial y^2} \quad (3.2.6)$$

$$\frac{\partial C}{\partial t} = \frac{1}{sc} \frac{\partial^2 C}{\partial y^2} \quad (3.2.7)$$

with initial and boundary conditions

$$u = \theta = C = 0, \quad y \geq 0, t = 0$$

$$u = 0, \theta = \begin{cases} t, & 0 < t \leq 1 \\ 1 & t > 1 \end{cases} = tH(t) - (t-1)H(t-1), C = t, \quad y = 0, \quad t > 0$$

$$u \rightarrow 0, \theta \rightarrow 0, C \rightarrow 0 \quad \text{as } y \rightarrow \infty, t > 0 \quad (3.2.8)$$

Where, H(.) is Heaviside unit step function.

3.2.4 Solution of the Model

Taking Laplace transform of equations (3.2.5) to (3.2.7) with initial and boundary conditions (3.2.8)

$$\bar{\theta} = \frac{1-e^{-s}}{s^2} e^{-y\sqrt{Prs}} \quad (3.2.9)$$

$$\bar{C} = \frac{e^{-y\sqrt{Scs}}}{s^2} \quad (3.2.10)$$

$$\bar{u}(y, s) = Gr(1 - e^{-s})F(s) + Gm G(s) \quad (3.2.11)$$

where,

$$F(y, s) = F_1(y)F_2(y, s) \quad (3.2.12)$$

$$G(y, s) = G_1(y, s)G_2(y, s) \quad (3.2.13)$$

$$F_1(s) = \frac{1}{\alpha Pr} \frac{1}{m_2 s} \frac{m_2}{(s+m_1)^2 - m_2^2}, \quad (3.2.14)$$

$$F_2(y, s) = F_3(y, s) - F_4(y, s) \quad (3.2.15)$$

$$F_3(y, s) = \frac{1}{s} e^{-y\sqrt{\frac{cs+b}{\alpha s+1}}} \quad (3.2.16)$$

$$F_4(y, s) = \frac{e^{-y\sqrt{Prs}}}{s} \quad (3.2.17)$$

$$G_1(s) = \frac{1}{\alpha Sc} \frac{1}{m_4 s} \frac{m_4}{(s+m_3)^2 - m_4^2} \quad (3.2.18)$$

$$G_2(y, s) = F_3(y, s) - G_3(y, s) \quad (3.2.19)$$

$$G_3(y, s) = \frac{e^{-y\sqrt{Scs}}}{s} \quad (3.2.20)$$

$$m_1 = \frac{Pr-c}{2\alpha Pr} \quad (3.2.21)$$

$$m_2 = \frac{\sqrt{(Pr-c)^2 + 4\alpha b Pr}}{2\alpha Pr} \quad (3.2.22)$$

$$m_3 = \frac{Sc-c}{2\alpha Sc} \quad (3.2.23)$$

$$m_4 = \frac{\sqrt{(Sc-c)^2 + 4\alpha b Sc}}{2\alpha Sc} \quad (3.2.24)$$

3.2.4.1 Solutions for plate with ramped wall temperature

Taking Inverse Laplace transform of equations (3.2.9) and (3.2.10)

$$\theta(y, t) = \theta_1(y, t) - \theta_1(y, t-1)H(t-1) \quad (3.2.25)$$

$$C(y, t) = \left(\frac{y^2 Sc}{2} + t\right) \operatorname{erfc}\left(\frac{y\sqrt{Sc}}{2\sqrt{t}}\right) - \frac{y\sqrt{Sc}t}{2\sqrt{\pi}} e^{-\frac{y^2 Sc}{4t}} \quad (3.2.26)$$

$$u = Gr f(y, t)H(y, t) - f(y, t)H(t-1) + Gm g(y, t) \quad (3.2.27)$$

where,

$$\theta_1(y, t) = \left(\frac{y^2 Pr}{2} + t\right) \operatorname{erfc}\left(\frac{y\sqrt{Pr}}{2\sqrt{t}}\right) - \frac{y\sqrt{Pr}t}{2\sqrt{\pi}} e^{-\frac{y^2 Pr}{4t}} \quad (3.2.28)$$

Inverse Laplace transform of equations (3.2.14) and (3.2.18) is $f_1(t)$ and $g_1(t)$

$$f_1(t) = \frac{1}{bm_2} [m_1 \sinh(m_2 t) + m_2 \cosh(m_2 t)] e^{-m_1 t} - \frac{1}{b} \quad (3.2.29)$$

$$g_1(t) = \frac{1}{bm_4} [m_3 \sinh(m_4 t) + m_4 \cosh(m_4 t)] e^{-m_3 t} - \frac{1}{b} \quad (3.2.30)$$

Inverse Laplace transform of equation (3.2.16), (3.2.17) and (3.2.20) is $f_3(y, t)$, $f_4(y, t)$ and $g_3(y, t)$

$$f_3(y, t) = \frac{c}{\alpha} e^{-t/\alpha} \int_0^\infty \operatorname{erfc}\left(\frac{y}{2\sqrt{z}}\right) e^{-c/\alpha z} I_0\left(\frac{2}{\alpha}\sqrt{(c-\alpha b)zt}\right) dz + \frac{b}{\alpha} \int_0^\infty \int_0^t \operatorname{erfc}\left(\frac{y}{2\sqrt{z}}\right) e^{-\frac{cz+s}{\alpha}} I_0\left(\frac{2}{\alpha}\sqrt{(c-\alpha b)zs}\right) ds dz \quad (3.2.31)$$

where,

I_0 is modified Bessel function of the first kind of order zero.

$\operatorname{erfc}(g)$ is complementary error function.

$$f_4(y, t) = \operatorname{erfc} \left(\frac{1}{2} \sqrt{\frac{Pr}{t}} y \right) \quad (3.2.32)$$

$$g_3(y, t) = \operatorname{erfc} \left(\frac{1}{2} \sqrt{\frac{Sc}{t}} y \right) \quad (3.2.33)$$

$$f_2(y, t) = f_3(y, t) - f_4(y, t) \quad (3.2.34)$$

$$g_2(y, t) = f_3(y, t) - g_3(y, t) \quad (3.2.35)$$

$$f(y, t) = f_1(t) * f_2(y, t) = \int_0^t f_1(t-s) f_2(y, s) ds \quad (3.2.36)$$

$$g(y, t) = g_1(t) * g_2(y, t) = \int_0^t g_1(t-s) g_2(y, s) ds \quad (3.2.37)$$

3.2.4.2 Solutions for plate with isothermal temperature

In this case, the initial and boundary conditions are the same excluding Eq. (3.2.8) that becomes $\theta = 1$ at $y = 0, t \geq 0$. Thus expression for velocity and temperature profiles are obtained with isothermal conditions which is given as below.

$$\theta(y, t) = \operatorname{erfc} \left(\frac{1}{2} \sqrt{\frac{Pr}{t}} y \right) \quad (3.2.38)$$

$$u = f_5(y, t)H(t) + Gm g(y, t) \quad (3.2.39)$$

Where

$$F_5(y, s) = F_6(s).F_2(y, s) \quad (3.2.40)$$

$$F_6(s) = \frac{1}{\alpha Pr m_2} \frac{m_2}{(s+m_1)^2 - m_2^2} \quad (3.2.41)$$

Inverse Laplace transform of equation (3.2.41) is

$$f_6(t) = \frac{1}{Pr \alpha m_2} \sinh(m_2 t) e^{-m_1 t} \quad (3.2.42)$$

Inverse Laplace transform of equation (3.2.40) is

$$f_5(y, t) = f_6(t) * f_2(y, t) = \int_0^t f_6(t-s) f_2(y, s) ds \quad (3.2.43)$$

From velocity, temperature and concentration fields, the expressions for Nusselt number, Skin friction and Sherwood number can be easily determined. They are measures of the heat transfer rate and shear stress at the boundary.

3.2.4.3 Nusselt number:

The Nusselt number Nu can be written as

$$N_u = -\left(\frac{\partial\theta}{\partial y}\right)_{y=0} \quad (3.2.44)$$

Using the equation (3.2.17), It is obtained the Nusselt number for Ramped wall temperature

$$N_u = \left[\frac{1}{2} \sqrt{\frac{tPr}{\pi}} H(t) - \frac{1}{2} \sqrt{\frac{(t-1)Pr}{\pi}} H(t-1) \right] \quad (3.2.45)$$

Using the equation (3.2.38), It is obtained the Nusselt number for isothermal temperature

$$Nu = \sqrt{\frac{Pr}{\pi t}} \quad (3.2.46)$$

3.2.4.4 Sherwood number:

Sherwood number is defined and denoted by the formula

$$s_h = -\left(\frac{\partial C}{\partial y}\right)_{y=0} \quad (3.2.47)$$

Using the equation (3.2.18), It is obtained the Sherwood number for Ramped wall temperature

$$s_h = \left[\frac{1}{2} \sqrt{\frac{tSc}{\pi}} \right] \quad (3.2.48)$$

3.2.4.5 Skin friction:

Skin friction, in dimensionless form, is

$$\tau_w(t) = \tau(y, t) \text{ at } y = 0 \quad (3.2.49)$$

Where the shear stress $\tau(y, t)$ can be written as

$$\tau(y, t) = \left(1 + \alpha \frac{\partial}{\partial t}\right) \frac{\partial u}{\partial y} \quad (3.2.50)$$

Using the equation (3.2.37), expression for Skin friction of ramped temperature can be written as,

$$\tau(y, t) = Gr F_6(y, t)H(t) - F_6(y, t - 1)H(t - 1) + Gm G_4(y, t) \quad (3.2.51)$$

Where

$$F_6(y, t) = \int_0^t I_1(t - s) \left. \frac{df_6}{dy} \right|_{y=0} dt \quad (3.2.52)$$

$$G_4(y, t) = \int_0^t I_2(t - s) \left. \frac{dg_4}{dy} \right|_{y=0} dt \quad (3.2.53)$$

$$I_1(t) = f_1(t) + \frac{1}{Pr m_2} \sinh(m_2 t) e^{-m_1 t} \quad (3.2.54)$$

$$I_2(t) = g_1(t) + \frac{1}{Sc m_4} \sinh(m_4 t) e^{-m_3 t} \quad (3.2.55)$$

3.2.5 Results and Discussion of the Problem

Effects of several involved physical parameters are described in Figures (3.2.2) to (3.2.12) on velocity, temperature and concentration profiles discussed. Figure 3.2.2 shows effect of Second grade fluid parameter α on velocity profiles for different values of y for both thermal conditions. In both thermal boundary condition, it is seen that velocity decrease with increase in α throughout the flow field. Figure 3.2.3 shows the effect of the magnetic field on the motion of the fluid. For both heating cases, velocity decreased with increase in magnetic parameter M . Physically, presence of magnetic parameter generates electric field in the flow, this implies that magnetic field has retarding effect on velocity profiles. This is due to point that the application of a magnetic field to electric conducting fluid gives increase to a resistive-type force (Lorentz force) on the fluid in the boundary layer, which slow down the motion of the fluid. This result has a significant role in large number of industrial applications, particularly in favor to solidification processes such as casting and semiconductor single crystal growth applications. The influence of the thermal Grashof number Gr and mass Grashof number Gm is shown in Figure 3.2.4 and Figure 3.2.5. It is observed that velocity increases with increase in Gr and Gm for both thermal cases. As predictable, the motion of the fluid rises and the top value is more distinctive due to growth in the thermal and mass buoyancy force.

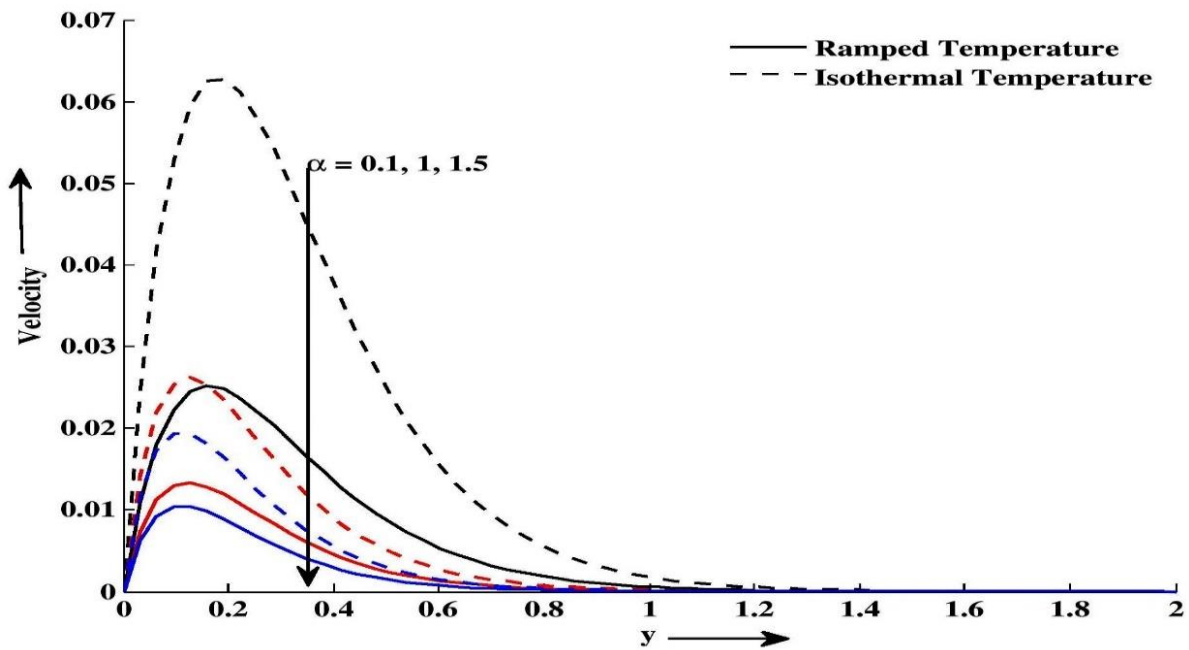


Figure 3.2.2: Velocity profile u for different values of y and α at $M = 5, Pr = 10, Sc = 6.2, k = 0.8, Gr = 7, Gm = 5$ and $t = 0.4$.

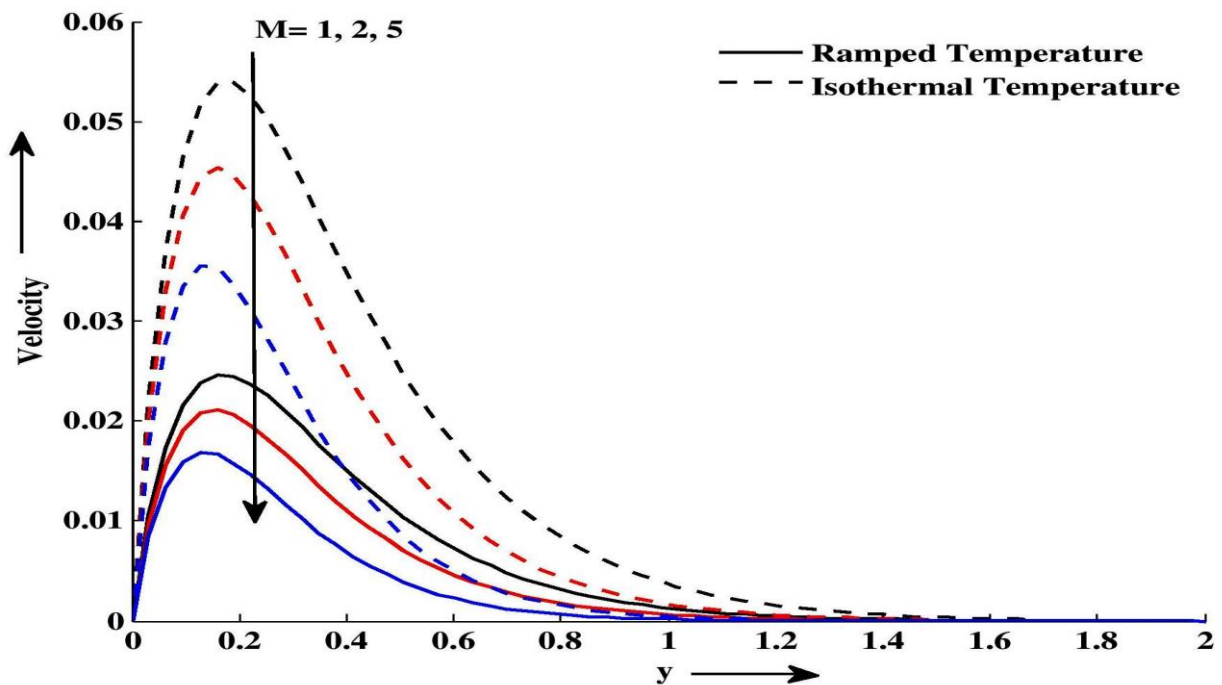


Figure 3.2.3: Velocity profile u for different values of y and M at $\alpha = 0.6, Pr = 10, Sc = 6.2, k = 0.8, Gr = 7, Gm = 5$ and $t = 0.4$.

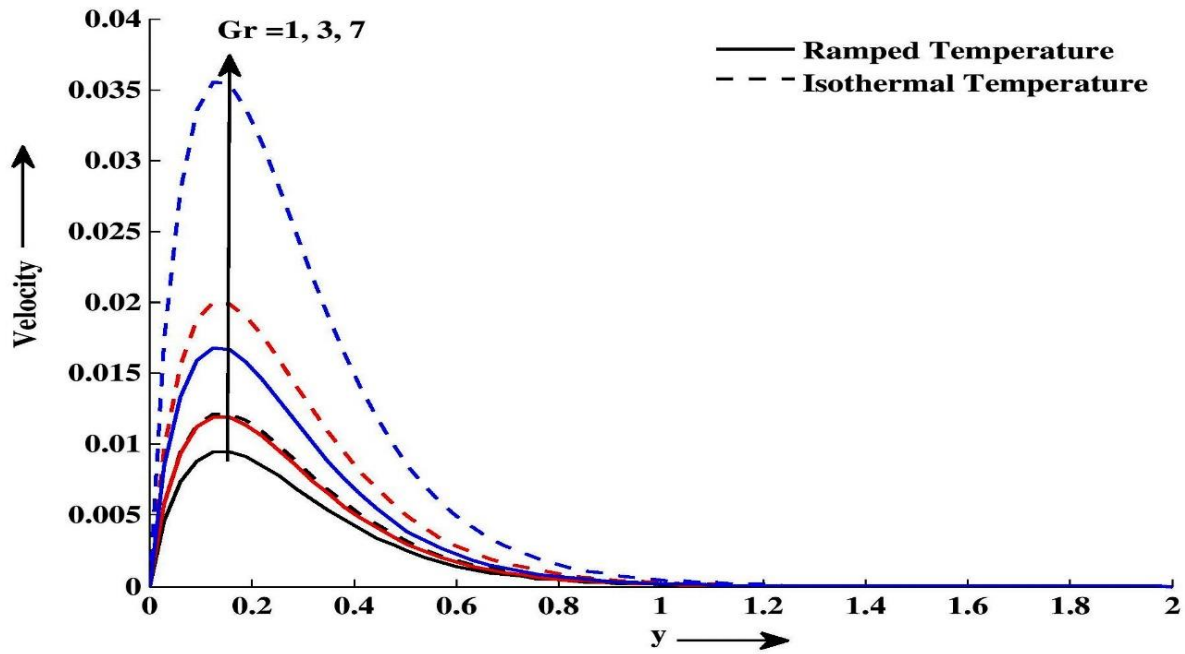


Figure 3.2.4: Velocity profile u for different values of y and Gr at $M = 5, Pr = 10, Sc = 6.2, k = 0.8, Gm = 5, \alpha = 0.6$ and $t = 0.4$

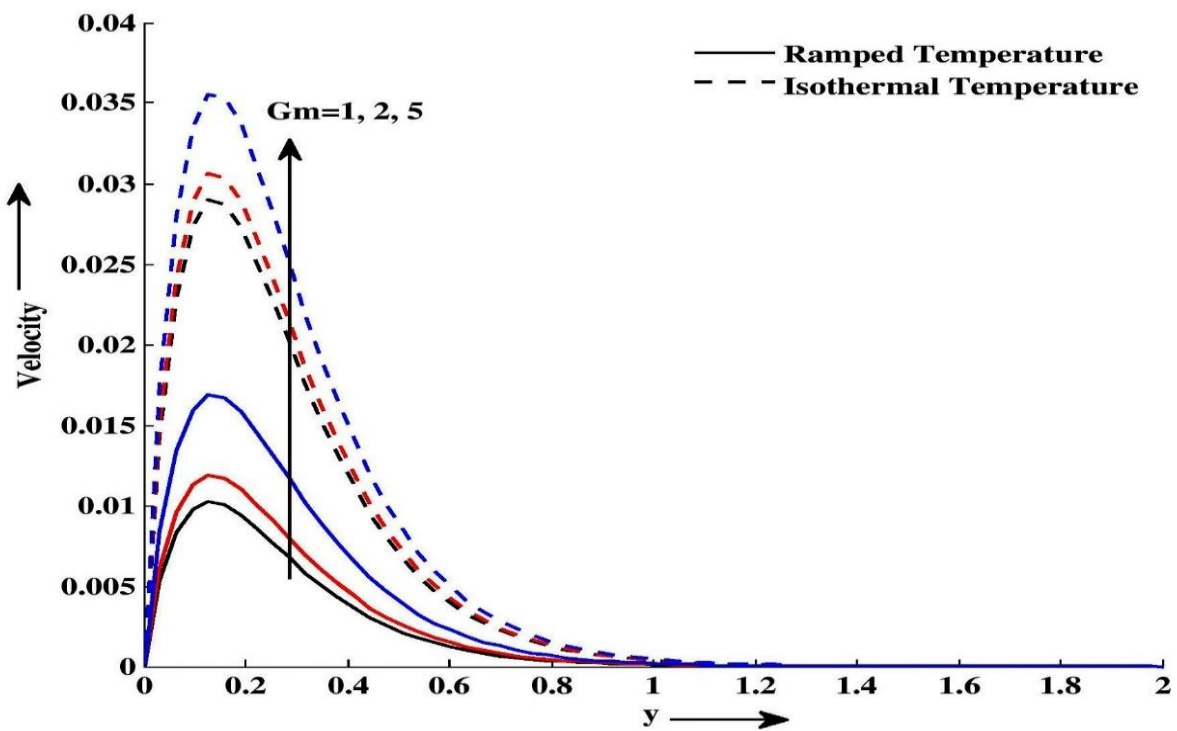


Figure 3.2.5: Velocity profile u for different values of y and Gm at $M = 5, Pr = 10, Sc = 6.2, k = 0.8, Gr = 7, \alpha = 0.6$ and $t = 0.4$

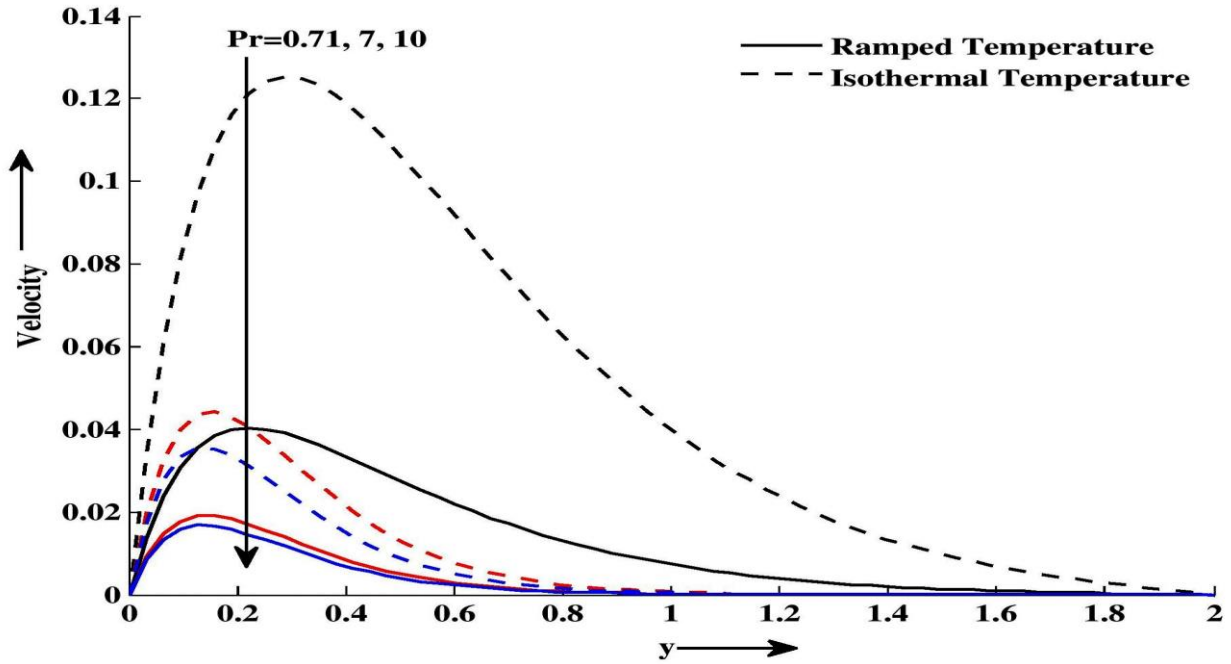


Figure 3.2.6: Velocity profile u for different values of y and Pr at $M = 5, \alpha = 0.6, Sc = 6.2, k = 0.8, Gr = 7, Gm = 5$ and $t = 0.4$

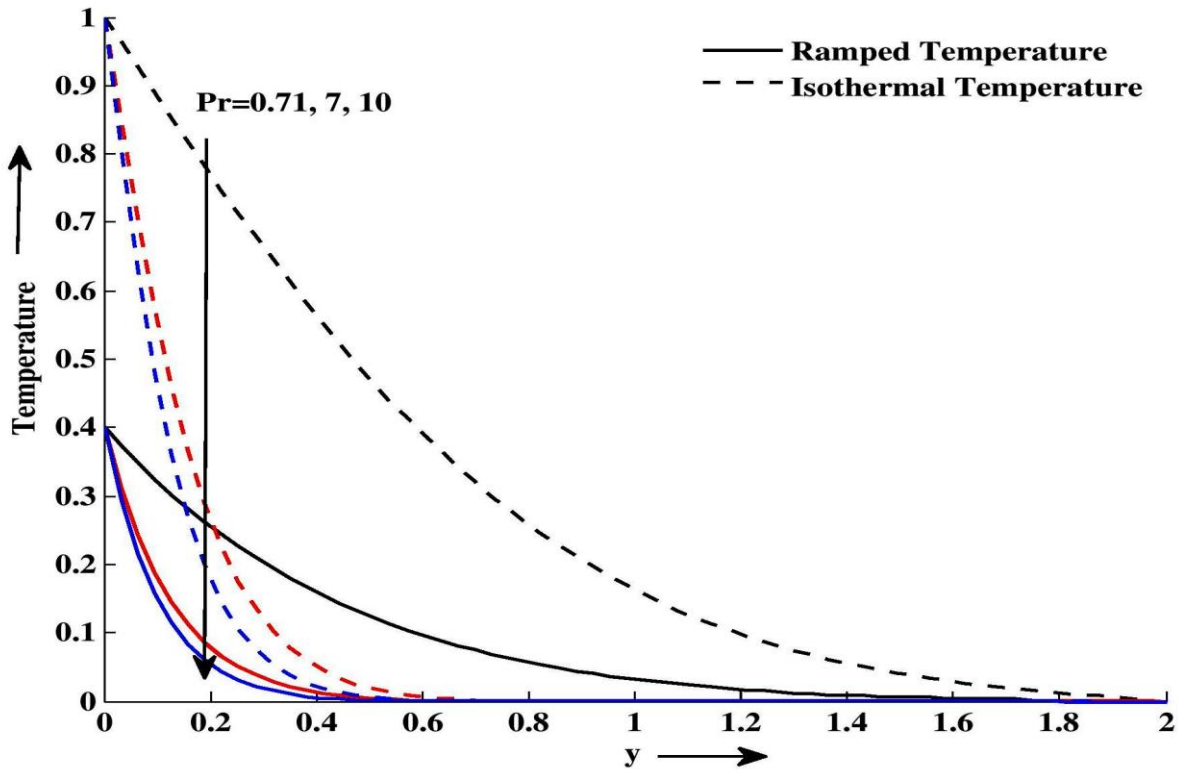


Figure 3.2.7: Temperature profile u for different values of y and Pr at $t = 0.4$.

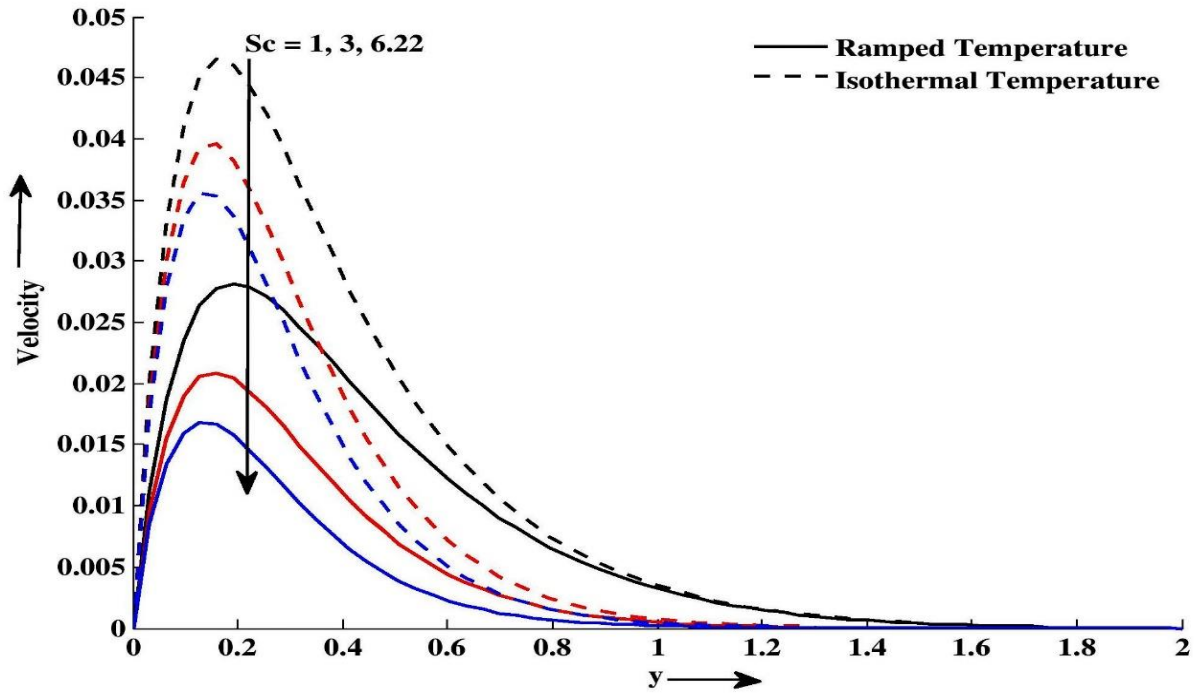


Figure 3.2.8: Velocity profile u for different values of y and Sc at $M = 5, Pr = 10, \alpha = 0.6, k = 0.8, Gr = 7, Gm = 5$ and $t = 0.4$

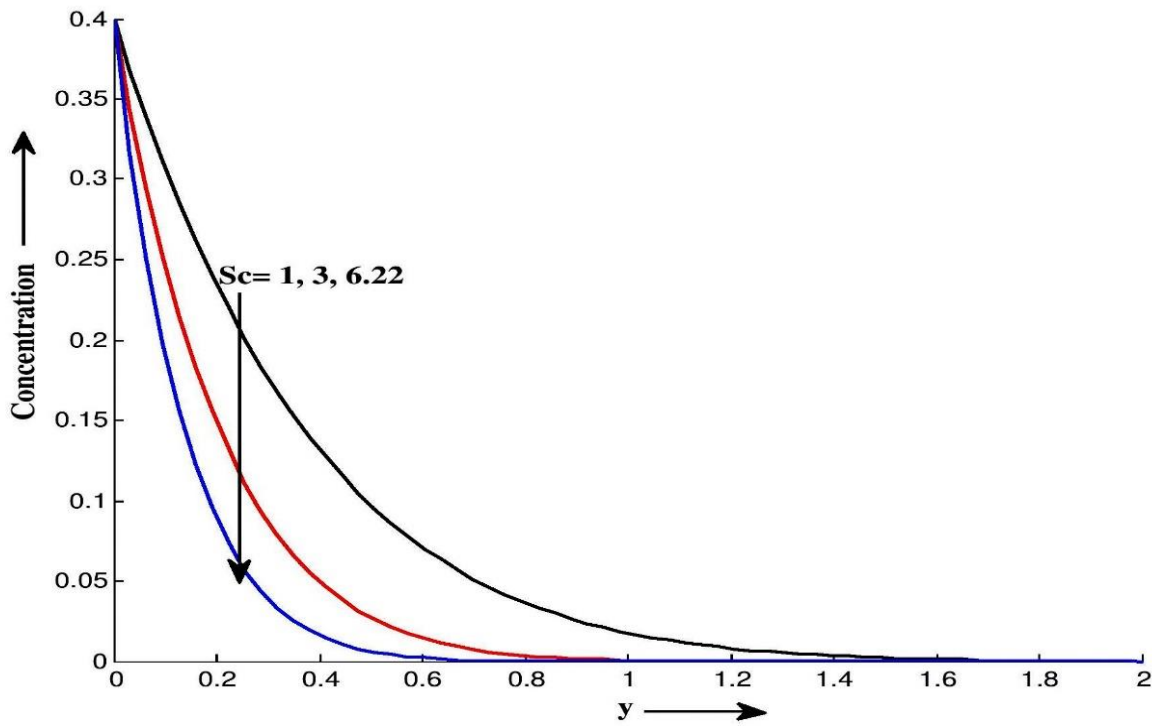


Figure 3.2.9: Concentration profile u for different values of y and Sc at $t = 0.4$

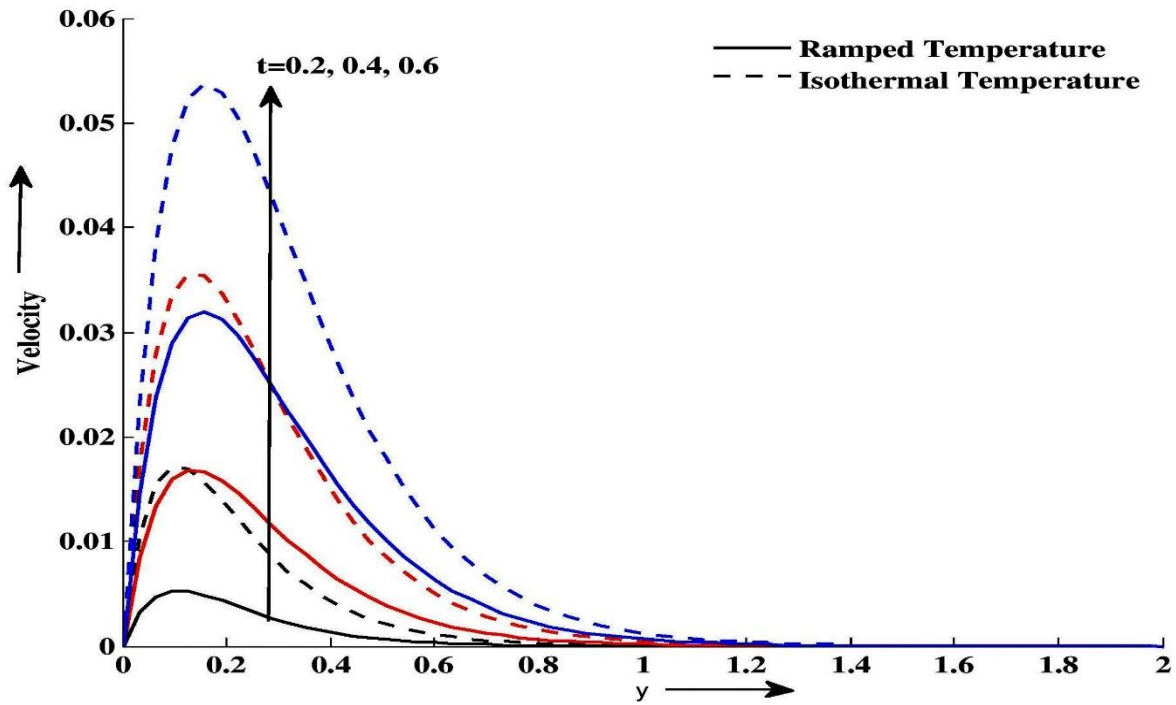


Figure 3.2.10: Velocity profile u for different values of y and t , at $M = 5, Pr = 10, Sc = 6.2, k = 0.8, Gr = 7, Gm = 5$ and $\alpha = 0.6$

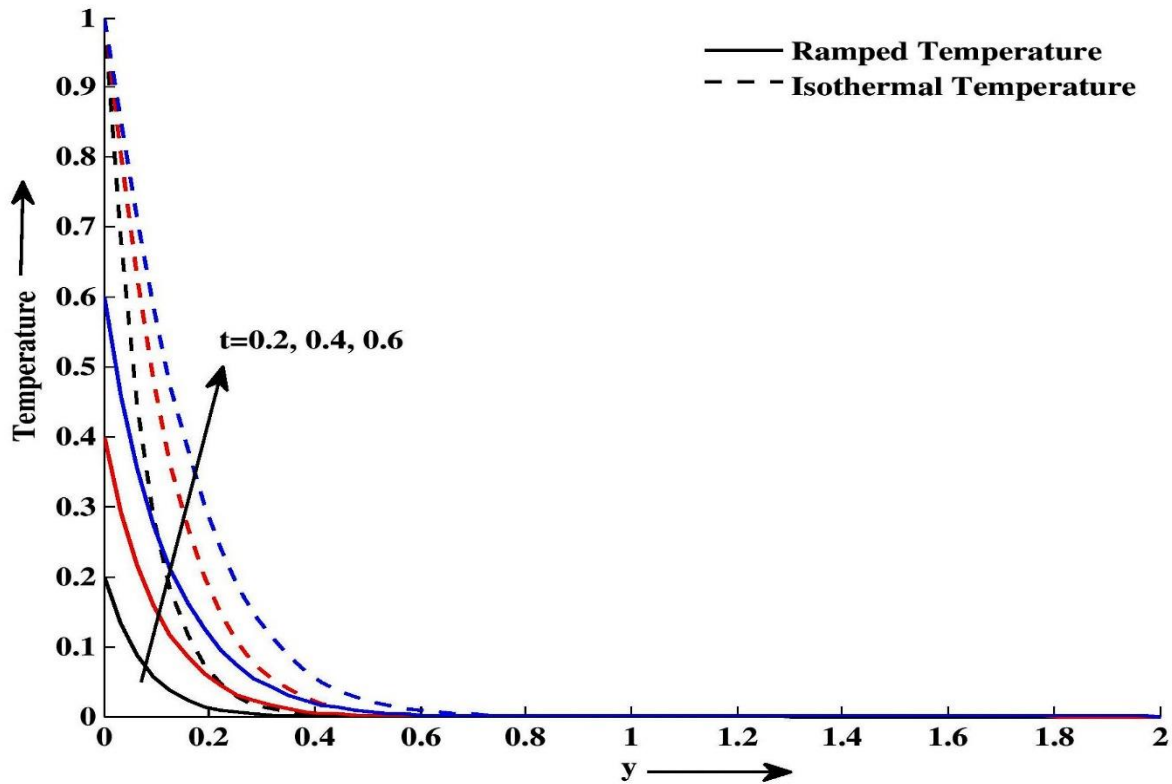


Figure 3.2.11: Temperature profile u for different values of y and t at $Pr = 10$

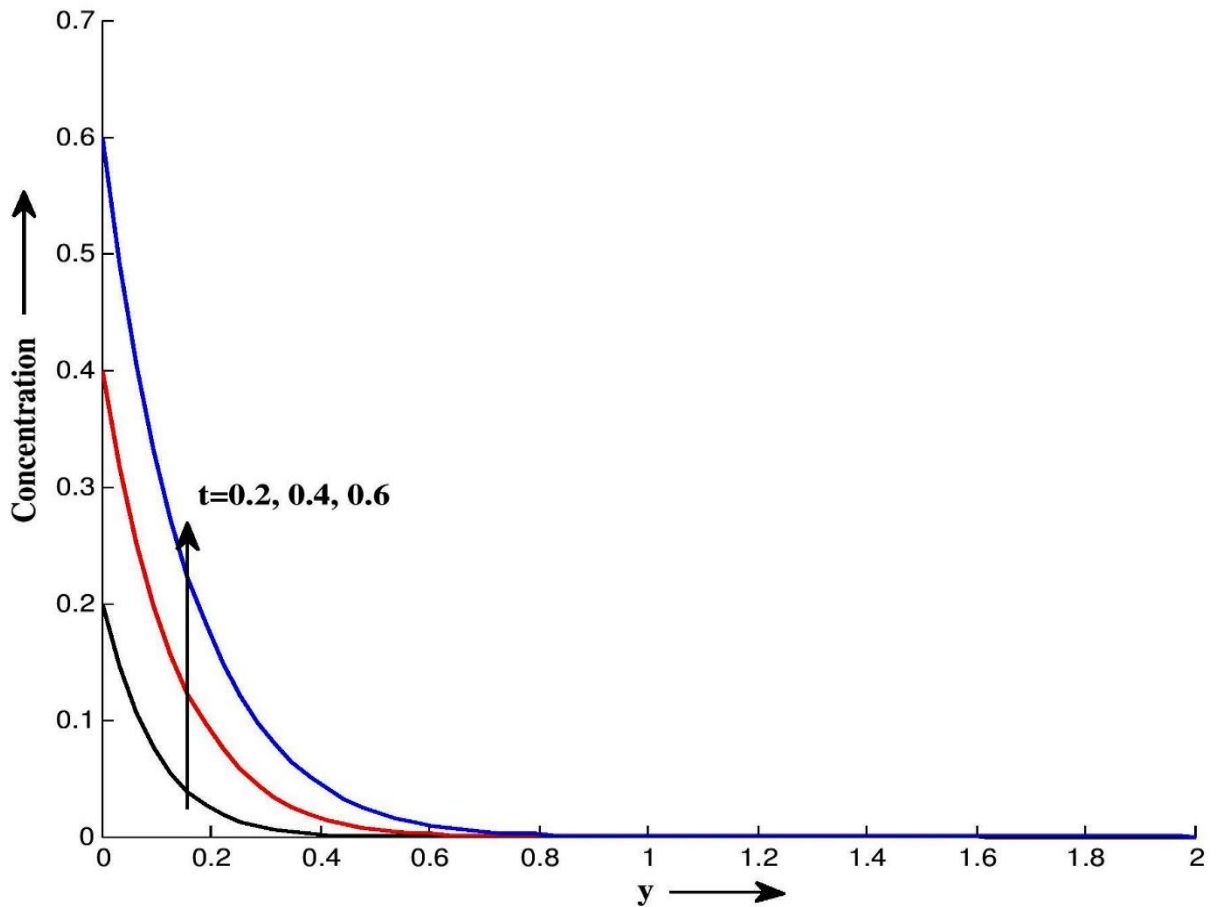


Figure 3.2.12: Concentration profile u for different values of y and t at $Sc = 6.2$.

Figure 3.2.6 and Figure 3.2.7 show the effect of Prandtl number Pr on velocity and temperature profiles for different values of y . In both heating cases, it is identified that momentum and heat transfer of fluid decrease tendency with Prandtl Number. In Figure 3.2.8 and Figure 3.2.9, velocity and concentration profiles are displayed with the variations in Schmidt number. It is observed that momentum and mass transfer decreases with increase in Schmidt number in both thermal cases. Physically, increase in Sc results in increased kinematic viscosity which in turn reduces molecular diffusion, there for fluid velocity decrease. Physically, it is justified because for large Sc , the fluid becomes denser. The concentration of the boundary layer decreases till it achieves the least value i.e. zero at the end of the boundary layer. Figure 3.2.10 to Figure 3.2.12 shows the effect of time on velocity, temperature and concentration for the both thermal cases respectively. It is seen that, velocity, temperature and concentration profile increase with increase in time.

3.2.6 Concluding Remark

The most important concluding remarks can be summarized as follows:

- The velocity, temperature and concentration distributions attains a maximum value in the neighborhood of the plate and then decreased properly to approach the free stream value.
- For both thermal plates, Second grade fluid parameter α , magnetic field parameter M tends to reduce fluid motion throughout the flow field.
- For both thermal cases, velocity of fluid decreased with increase in Pr and Sc throughout the flow field.
- Prandtl number tends to reduce Heat transfer process, whereas Schmidt number reduced mass transfer process.
- Flow, heat and mass transfer increased with time t .